High sensitivity absorption spectroscopy of acetylene near 1.2 μm

O.M. Lyulin, S. Kassi, A. Campargue

Journal of Quantitative Spectroscopy and Radiative Transfer

High sensitivity absorption spectroscopy of acetylene near 1.2 μm

--Manuscript Draft--

Manuscript Number:	JQSRT-D-21-00249R1
Article Type:	VSI:HITRAN2020
Keywords:	acetylene; C2H2; effective Hamiltonian; CRDS; spectroscopic database; HITRAN
Corresponding Author:	alain Campargue cnrs Saint Martin d'Hères, France
First Author:	alain Campargue
Order of Authors:	alain Campargue
	Oleg LYULIN
	Samir Kassi
Abstract:	The weak high-resolution absorption spectrum of natural acetylene has been recorded by high sensitivity cavity ring down spectroscopy (CRDS) near 1.2 μm. The frequency scale of the spectra was obtained by coupling the CRDS spectrometer to a self-referenced frequency comb. The room temperature recordings, performed at a pressure of 10.0 Torr, cover the 8210-8670 cm -1 spectral interval. A list of more than 11000 lines was constructed in the region. The smallest intensity values are on the order of 10 -29 cm/molecule which is more than two orders of magnitude smaller than previous measurements by Fourier transform spectroscopy (FTS). More than 2600 lines were rovibrationally assigned using previous observations and predictions based on the effective operator approach. They include 2270, 338 and 28 absorption lines of 12 C 2 H 2 , 12 C 13 CH 2 and 12 C 2 HD, respectively, belonging to a total of 52 vibrational bands, thirty-six of them being newly reported. For comparison, the HITRAN2016 database provides line parameters of only two 12 C 2 H 2 bands in the same region. Spectroscopic parameters of the upper vibrational levels were derived from standard band-by-band fits of the line positions (typical rms values of the (obs.-calc.) deviations are better than 0.002 cm –1). The vibrational transition dipole moment squared and Herman-Wallis coefficients of 39 bands were derived from a fit of the intensity values measured in this work combined with previous FTS data for the strongest bands. A recommended list is constructed in the region using calculated line parameters for the unperturbed bands and experimental positions and intensities for the others. The recommended list including a total of 3139 transitions will help to complete acetylene spectroscopic databases in the near-infrared.
Suggested Reviewers:	Valery Prevalov vip@iao.ru
	David Jacquemart david.jacquemart@upmc.fr
	Jean Van der Auwera jauwera@ulb.ac.be
Response to Reviewers:	see attached file

Dear Sir,
Please find the revised version of our paper:
High sensitivity absorption spectroscopy of acetylene near 1.2 µm

by O. M. Lyulin , S. Kassi and A. Campargue

that we submit to the JQSRT HITRAN2020 SI.
We thank the two reviewers for their useful comments and hope that the amended version is now suitable for publication in JQSRT.

Regards,
Alain Campargue

Response to the reviewers

Ref: JQSRT-D-21-00249
Title: **High sensitivity absorption spectroscopy of acetylene near 1.2µm**
by O. Lyulin, S. Kassi, and A. Campargue.

We thank the reviewers for their careful reading of the paper and useful comments.

Reviewer 1

In the reviewed paper the weak high-resolution absorption spectrum of natural acetylene has been recorded by high sensitivity cavity ring down spectroscopy (CRDS) in the 8210-8670 cm^{-1} spectral interval. About 2600 lines from more than 11000 observed lines were rovibrationally assigned to three isotopologues of this molecule. The line positions and line intensities were measured. Where it was possible the spectroscopic constants were fitted to the measured line positions and vibrational transition moments squared and Herman-Wallis parameters were fitted to the observed line intensities. Basing on this modeling the acetylene line list for the considering spectral region was prepared. The article can be accepted for publication in The Journal of Quantitative Spectroscopy and Radiative Transfer provided the following comments are addressed.

Minor comments

1) Page 10, the last sentence "… it might be that part of the lines left unassigned could not be identified because their measured positions deviate considerably compared to their ASD values"
The authors have assigned about 3500 methane lines in their spectrum. So among the unassigned lines could be the ethylene lines. It is necessary to discuss this. It is indeed an important question as experimental intensity values are weighted according to their error bars in the fit of the EDM parameters.

Indeed, in our previous CRDS studies around 6000 cm^{-1} where the acetylene spectrum is weak and ethylene spectrum is strong, we could identify many lines due to ethylene present as an impurity in our sample. The identification relied on the comparison with an FTS spectrum recorded by Jean Vander Auwera at ULB which is reproduced here (left-hand Figure). The upper limit of this FTS spectrum is 8400 cm^{-1}, so it does not cover the 8400-8680 cm^{-1} range of our recordings. Nevertheless, no absorption lines appear below 8400 cm^{-1} where many lines remain unassigned in our spectrum (right-hand Figure). So we do not expect a significant contribution of ethylene. We have nevertheless modified our text: *"Although we cannot exclude that part of these unassigned lines are due impurities (e.g. ethylene), the majority of these lines are believed to be due to 12C2H2. "*

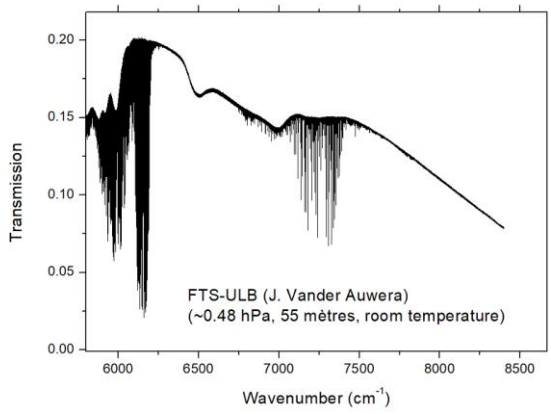

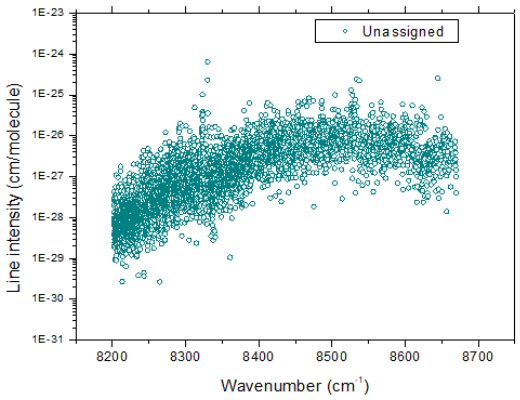

2) Fig.6 and Table 2
The bands v2+v3+5v41 and 2v2+(6v4+v5)1II look strongly perturbed. Did authors analyze the perturbation mechanism?

In Fig.6 the deviation of these two bands are much larger than for other bands. It just means that there are some missing parameters in the effective Hamiltonian used for generating ASD-1000. So including these bands in the fit of the effective Hamiltonian will make very useful correction in the future version of the ASD-1000 database. The following sentence has been added in the text: *"These important deviations probably reveal the need to include some additional parameters in the effective Hamiltonian used for the generation of ASD. The evidenced deviations will be thus valuable to improve future versions of ASD. "*

3) Fig. 9
What is the reason for the "scattering" of the intensities of some lines (misassignment, blending, perturbation)?
The main reason of the intensity scattering is the weakness of the lines. At this level of sensitivity, the spectrum includes many hot bands and the corresponding weak lines are often blended.

4) Fig. 8
In my computer the red dashed line looks like red solid line.
On this new version, it should be clearer.

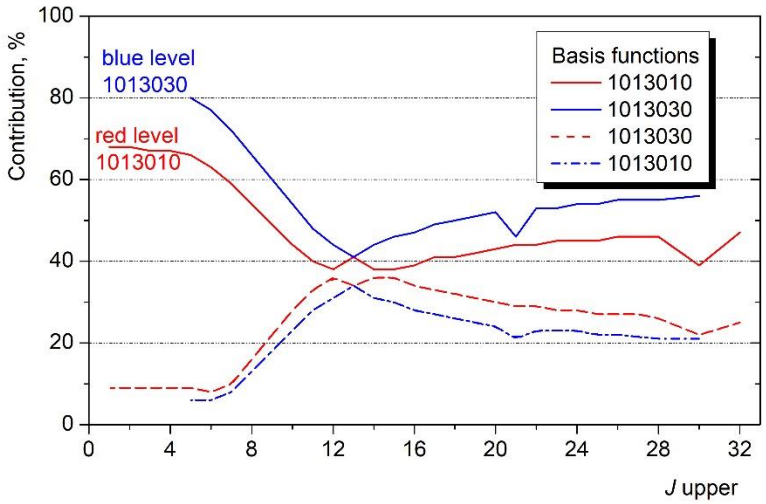

5) Eq.(2)
In my computer instead of "h" I see sign of square.
In our docx file, there is no problem

6) Eq.(3)
After this equation it is necessary to define s like s = 1 if sign(ΔK)=1, s = -1 if sign(ΔK)=-1.
Following recommendation, we added in the text "*s* = +1 and -1 for positive and negative values of *ΔK*, respectively".

-**Reviewer 2**

The work presented in the manuscript is relevant for publication in JQSRT. The authors present new measurements based on a single pressure CRDS spectrum analysis using a flow of acetylene regulated at 10.00 Torr. A commercial sample has been used so that measurements of line intensities are supposed to be in natural abundances. Around 8000 transitions of acetylene (including minor acetylene isotopologues) have been studied between 8210 and 8670 cm-1. Energy levels constants, R02 and HW parameters have been derived for several bands in order to generate a recommended line list for around 3000 assigned transitions including bands previously measured.

I have general issues that need to be considered:

I- The authors wrote about 3 supplementary files containing measured data and recommended line list but no file has been submitted. Please submit them to JQSRT in order to pursue the revision.

We apologize for this mistake. The three supplementary files are attached to the revised version.

II- The authors should explain better how the recommended line list is constructed. I will be more specific below. The fact that the supplementary files were missing did not help to understand what has been done.

See below our answers

III- No serious comparison between present measurements and those from literature are performed. I noticed that one of your highlights is « Comparison to literature data is discussed ».

The reviewer limits the "literature" to previous experimental studies but the ASD is an important work available in the literature which has been carefully compared to our results. We believe that there is no more "serious" discussion in the region. In our series of papers on acetylene, we carefully and systematically compared our measurements to previous data and in particular to HITRAN database.

In the presently studied region, the most relevant previous experimental study is our FTS study of Ref. [10]. Most of the line parameters of this study were transferred to our list as the corresponding lines are generally saturated in our CRDS spectrum. So a comparison to Ref. [10] is not relevant for the present contribution BUT in Ref. [10] we reported the following discussion about the comparison to HITRAN:

5. Comparison with the HITRAN 2012 database

As illustrated in Fig. 3, the HITRAN line list [15] includes only two bands, $\nu_1+\nu_2+\nu_3$ and $\nu_1+2\nu_2+(\nu_4+\nu_5)^{0+}$, with positions and intensities from Vander Auwera et al. [17] and Jacquemart et al. [19], respectively. The overall agreement is satisfactory. As an example, for the $J<30$ positions of the strong $\nu_1+\nu_2+\nu_3$ band, the average difference and *rms* deviation are -1.1×10^{-4} cm^{-1} and 5.2×10^{-4} cm^{-1}, respectively. In the absence of measurements for some transitions, the HITRAN line parameters were interpolated and some high J line parameters extrapolated. For instance, the HITRAN list of the $\nu_1+2\nu_2+(\nu_4+\nu_5)^{0+}$ band includes the P(30)–R(30) transitions while the original measurements by Vander Auwera et al. were limited to the P(21)–R(21) transitions [17]. Our measurements of higher J transitions allow checking the quality of the high J extrapolation based on the band parameters derived in Ref. [17]. Differences on the order of 0.01 cm^{-1} are noted for the highest J values (around $J=35$) for the two bands included in HITRAN. A similar situation was found in the 7000–7500 cm^{-1} region [14]. The intensity comparison with HITRAN database shows a good agreement with average relative deviations better than 5% and 10% for the $\nu_1+\nu_2+\nu_3$ and $\nu_1+2\nu_2+(\nu_4+\nu_5)^{0+}$ bands, respectively.

Fig 5 is not a serious comparison and Table 3 compares only number of lines and bands in various sources.

We have never claimed that Fig 5 was a comparison of line parameters but just the contents of different data sets. In the submitted version, we simply wrote: "*An overview of our assigned list is presented in Fig. 5 and compared to the HITRAN2016 list and to the previous FTS list of Ref. [10]"* . Fig. 5 doesn't present the comparison

How your present measurements are matching with those of Ref 10 or the one used in HITRAN for intense bands.

See above copy of the paragraph devoted to the HITRAN comparison included in Ref. [10].

We have added in the text: *"Note that the HITRAN2016 includes only two bands and that the position and intensity comparisons between the FTS values of Ref. [10] and HITRAN2016 values were discussed in Ref. [10]."*

You wrote that present measurements are not accurate for line intensities greater than E-25 (did you discard them all for the fit of R02 and HW coefficients?).

Yes the FTS values were preferred for the strong lines (>1E-25) and we did not use the CRDS values. It is clearly indicated in the text: *"…we adopted for about 430 lines with intensity larger than 1×10^{-25} cm/molecule, the FTS line parameters of Ref. [10] obtained at a pressure of 42.4 Torr and an absorption pathlength of 48.3 m. The FTS source of the line parameters is indicated in the line list provided in the Supplementary Material I*."

It is a pity that the reviewer could not examine our sup mats because the lines transferred from Ref. [10] are tagged.

You present those measurements in Fig 5 (red symbols appears below HITRAN ones). Using the scale of Fig 5, comparisons look good between PW and HITRAN or Ref [10], but what is the difference in % for common transitions between your work and original source of HITRAN2016 (Jacquemart et al, JQSRT 2009 ;110 ;732-742) or Ref [10]? Cross-comparisons are very important and should be presented in some figure or Table or in the text by giving average discrepancy (with SD) for common measured transitions.

This is exactly what have been done in the above paragraph of Ref. [10]. This is not relevant in the present paper.

Specific issues :

- In the abstract: « The vibrational transition dipole moment squared and Herman-Wallis coefficients of 39 bands were derived from a fit of the measured intensity values. »

This is not clear whether measured intensities are referring to the present work or to the combination of present measurements and those of Ref 10.

The reviewer is right. The vibrational transition dipole moment squared and Herman-Wallis coefficients derived in this work rely not only on the present CRDS measurements but also include as input data our FTS measurements of Ref. [10].

We modified the statement. « *The vibrational transition dipole moment squared and Herman-Wallis coefficients of 39 bands were derived from a fit of the intensity values measured in this work* ***combined with previous FTS data for the strongest bands***»

- « In the case of isolated lines with intensity larger than 10-27 cm/molecule, a 5% value is a conservative estimate of the uncertainty on the line intensity ». What about lines with S > E-25 cm/molecule? I suppose they are given in supplementary material. You wrote that accuracy are degraded for these transitions, can you give an estimation of their accuracy? What about uncertainty of measurements for non-isolated transitions, can you give some estimation?

As said above and indicated in the text, the lines with intensities S > E-25 were mostly taken from ref. [10]- See Text just before Section 3: "*Consequently, we adopted for about 430 lines with*

intensity larger than 1×10^{-25} cm/molecule, the FTS line parameters of Ref. [10] obtained at a pressure of 42.4 Torr and an absorption pathlength of 48.3 m. The FTS source of the line parameters is indicated in the line list provided in the Supplementary Material I." In Ref. [10], we indicated that the average accuracy of the intensity measurements is about 5%, so the same as the value given for CRDS intensities larger than *1×10^{-75} cm/molecule*. The estimated transition uncertainties are given for every band in the last column of Table 2.

- « As a combined effect of perturbations and experimental uncertainties due to line overlapping and to the weakness of many bands, a significant number of line intensities had to be excluded from the fit. » Precise how many measurements did you remove (or % removed measurements).

It depends on the band and can reach a value of 50%. Again we apologize because the reviewer would have found in Supmat3, the relative intensity differences between measured and calculated values for every line and the weight given in the fit. One can also compare the number of fitted lines indicated for every band in Table 2 and the number of measured in the band lines indicated in the Table 1.

- « Even with a reduced input dataset, a satisfactory fit could not be achieved for a significant number of bands. In such cases, we provide only the vibrational transition moment squared value with a large uncertainty. ». What is the reduced dataset? Do you mean the fit of line profile (intensities) or the fit of R2 to get R02 and HW for each band?

We are speaking of an input dataset of a fit so it is clear that we are speaking of the fit of R02 and HW

How do you define that a fit is not satisfactory? In Table 2 you wrote when a fit of intensities failed… Does it correspond to band with no measurement of line intensities (Nexp =0, blank in Table 2) ? In that case how did you estimate R02 and the digit between parentheses (SD) for the band where there is no measurement?

The line intensities were measured for all bands and the column Nexp contains the number of fitted lines (No value is given when the fit fails). As usual in the fit of measured data, outliers are excluded to reach satisfactory agreement for the remaining data. In our case, we considered deviations of about 10% as satisfactory. The fit was considered unsatisfactory when even the identification of the outliers was problematic. However, even in these conditions, the fits were performed and rough vibrational dipole moment squared values were obtained. We have added in the foot note: ^{d} N_{exp} "*No value is given when the fit failed.*"

- You give in Table 2 uncertainty for each band. In the text you wrote: « In many cases, in view of the number of intensity values which were excluded, it seems that the obtained *rms* values overestimate the quality of the fits and we give in the last column of Table 2 our own estimation of the relative error bars of the intensities calculated with the obtained set of parameters. » I do not understand the argument. The more « outliers » you will remove, the best average rms you will get on the band. Maybe the authors wanted to use underestimate instead of overestimate since by looking to rms and uncertainty from Table 2, the uncertainty is systematically higher than rms. Also, why « relative error bars » ? Do you mean that accuracy is worst ? What is the meaning of uncertainty and relative error, compare to accuracy ? Uncertainty is used in the whole text without really know its signification.

No, indeed, readers considering our rms values will conclude that our fit is satisfactory while the good achieved rms values are due to the exclusion of a significant number of experimental values. So, indeed, the given *rms* values "overestimate" the real quality of the fit. This is why we give larger uncertainty values.

As concerns definitions, "relative error" is in %, "uncertainty" is not absolute contrary to "accuracy"

- In section 2 and 7, the authors wrote « normal isotopic abundances ». I suppose they mean natural isotopic abundances. Please correct as normal does not mean a lot.

We have performed this change (2 places) although we believe that “natural” is also unclear. Linda Brown (JPL) was refusing “natural” because indeed there is no “natural” isotopic abundance values (HITRAN values are arbitrary values which may strongly differ from values in “natural” materials). In other words, it means that the used sample is not supposed to be strongly enriched in one isotope, it is “normal”.

- Eq 3 for HL should be clarified. Are HL using Eq 3 the same than those using equations from Ref. [15,32]? Equation 3 is hard to apply, could you give examples?

$$L^{\Delta K}(J,K) = L^{\Delta K - s}(J,K+s)\left\{J\left(J+1\right) - K\left(K+s\right)\right\} = L^{\Delta K - s}(J,K+s)\left\{\left(J+1+Ks\right)\left(J-Ks\right)\right\}$$

Let us consider for example ΔJ=1, ΔK>1 (s=1)

For ΔK=1 Honl-London factor is

$$L^{\Delta K=1}(J,K) = \frac{\left(J+K+1\right)\left(J+K+2\right)}{2\left(J+1\right)}$$

Then, following recurrent expression, one obtains for ΔK=2

$$L^{\Delta K=2}(J,K) = L^{\Delta K=1}(J,K+1)\left\{\left(J+K+1\right)\left(J-K\right)\right\} = \frac{\left(J+K+2\right)\left(J+K+3\right)\left(J+K+1\right)\left(J-K\right)}{2\left(J+1\right)}$$

And ΔK=3

$$L^{\Delta K=3}(J,K) = L^{\Delta K=2}(J,K+1)\left\{\left(J+K+1\right)\left(J-K\right)\right\} =$$

$$= \frac{\left(J+K+3\right)\left(J+K+4\right)\left(J+K+2\right)\left(J-K-1\right)\left(J+K+1\right)\left(J-K\right)}{2\left(J+1\right)}$$

In the case of ΔK<-1 (s=-1)

ΔK=-1

$$L^{\Delta K=-1}(J,K) = \frac{\left(J-K+1\right)\left(J-K+2\right)}{2\left(J+1\right)}$$

ΔK=-2

$$L^{\Delta K=-2}(J,K) = L^{\Delta K=-1}(J,K-1)\left\{\left(J-K+1\right)\left(J+K\right)\right\} = \frac{\left(J-K+2\right)\left(J-K+3\right)\left(J-K+1\right)\left(J+K\right)}{2\left(J+1\right)}$$

ΔK=-3

$$L^{\Delta K=-3}(J,K) = L^{\Delta K=-2}(J,K-1)\left\{\left(J-K+1\right)\left(J+K\right)\right\} =$$

$$= \frac{\left(J-K+3\right)\left(J-K+4\right)\left(J-K+2\right)\left(J+K-1\right)\left(J-K+1\right)\left(J+K\right)}{2\left(J+1\right)}$$

Note that in ref. [10] there is mistype in the expression for ΔJ=1 ΔK=±3, there should be $\left(J \pm K+1\right)$ instead $\left(J \mp K+1\right)$.

- In Section 2, it's written « Overall, line centres and intensities were derived for a total of more than 11500 lines » . I believe it's better to write line positions and intensities. Centre is in French and we normally use line positions instead of « centre de raie ».

Done, even if we are not convinced. See for instance, the use of “line centers” in:
https://en.wikipedia.org/wiki/Spectral_line#Line_broadening_and_shift

- Figure 9 shows rotational dependence observed in this work and modeled using HW coefficients. For the two bands presented in the upper plots of Fig 9, the observed R2 values show clear rotational dependence that cannot be reproduced by HW (due to strong interactions between levels). Rigorously

you should speak about bands involving interacting levels (you wrote : The two upper panels are related to the $\nu_1+\nu_3+3\nu_4^1$ and $\nu_1+\nu_3+3\nu_4^3$ interacting bands presented in Fig. 8.).

Strictly speaking, the reviewer is right but the shortcut "interacting bands" is very convenient and understood by everybody. We have modified our text:

A similar situation was found for the $\nu_1+\nu_3+3\nu_4^1$ and $\nu_1+\nu_3+3\nu_4^3$ bands centered at 8330 cm^{-1} and 8329.3 cm^{-1}, respectively. The two principal contributions of the basic functions to the corresponding interacting upper states were obtained from the global effective modeling [8] and are plotted in **Fig. 8**

My comment is about your recommended line list, in such case what did you do? In section 6, authors wrote they used HW from Table 2. Did they also do it for the bands showing observed rotational dependences that cannot be reproduced by HW factors (Fig 9) ? If yes the uncertainty for this band will be much higher than 15% for high m values. The authors should add some comments in Section 6 for the case of such bands presenting strong rotational dependences that cannot be reproduced by HW factor.

The way used to construct the recommended line list is clearly indicated in the second paragraph of the section 6. For example, it is written: *"In the cases where the intensity fit failed or the measured intensity was significantly smaller than the calculated value, the measured value was transferred to the recommended line list with a "e" tag."* The choice between measured and calculated intensity values were made for each line after a careful scrutiny of the superposition of the measured and calculated line lists to the measured spectrum. Again we apologize because the reviewer would have found in Supmat3, the indication of the choice we made for each line.

- Correct English in « On the basic of the empirical parameters obtained from the measured positions and intensities, a line list was generated for each band listed in Table 2 at the reference temperature of 296 K ». Based on (or on the basis of the)…

Done.

- The number of acetylene transitions measured in this work and used to determine HW coefficients is missing. Ntot is the number of line (combination of this work and Ref 10) used to fit HW parameter for each band. You have to indicate how many are coming from literature in the case of the few bands already studied [HITRAN,Ref10]. You wrote that 430 line from Ref [10] have been used to replace present measurements for S > E-25 cm/molecule. What about the 2 strongest bands present in HITRAN, which measurement did you use to generate HW and R02 of Table 2 ? I found the following sentence: « Vibrational transition dipole moments squared and Herman-Wallis coefficients obtained from an unweighted fit of the experimental intensity values are reported in Table 2. ». Please clarify which measurements have been used to fit values of Table 2.

For line positions only positions measured in the present work have been used to deduce spectroscopic parameters of Table 1, am I right? Please confirm that only measured positions from this work have been used to retrieve parameters of Table 1.

By the way, the report of positions concerning the two strongest bands should refer to original works (Vander Auwera et al. Mol Phys 2002;100:3563-76 + Jacquemart et al, JQSRT 2009 ;110 ;732-742) used in HITRAN2016.

In all our contributions, we take a special care of the traceability of listed line parameters. Again the reviewer would have found in Supmat1, the information he/she requests. Sorry for the missing supmats.

The lines transferred from the Ref. [10] are marked in the Supmat1. The transferred positions and intensities have been used in the fits of the spectroscopic constants and HW factors. Here is a fragment of supmat1 for a band mixing FTS and CRDS line parameters:

(9) FTS: Lines added from Lyu16: JQSRT 2016;177:234–240

(1)	(2)	(3)	(4)	(5)	(6)	(7)	(8)								(9)
IC	Position Meas	Intensity Meas	Position Calc	O–C F	CD	E''	Assignement BJ VS	Upper			Lower				Source
261	8461.1335	0.8052E–24	8461.1335	0.01	0.70	647.1089	P5 ff	11110	1	0	00010	1	0		FTS
261	8463.6398	0.1942E–23	8463.6400	–0.20	0.94	635.3042	P4 ff	11110	1	0	00010	1	0		FTS
261	8466.1091	0.4922E–24	8466.1102	–1.12	–3.50	625.8602	P3 ff	11110	1	0	00010	1	0		FTS
261	8468.5369	0.5471E–24	8468.5441	–7.20*	–6.38	618.7770	P2 ff	11110	1	0	00010	1	0		FTS
261	8473.2759	0.7663E–24	8473.2767	–0.82	6.38	614.0444	Q1 fe	11110	1	0	00010	1	0		FTS
261	8473.2449	0.3189E–24	8473.2247	20.16*	17.78	618.7456	Q2 fe	11110	1	0	00010	1	0		FTS
261	8473.1469	0.3993E–24	8473.1468	0.14	1.28	625.7974	Q3 fe	11110	1	0	00010	1	0		FTS
261	8473.0419	0.7307E–25	8473.0428	–0.88	–0.19	635.1996	Q4 fe	11110	1	0	00010	1	0		
261	8472.3663	0.3890E–25	8472.3666	–0.28	–0.58	696.3085	Q8 fe	11110	1	0	00010	1	0		
261	8472.1323	0.6506E–25	8472.1324	–0.08	–0.47	717.4595	Q9 fe	11110	1	0	00010	1	0		
261	8471.5830	0.1331E–24	8471.5857	–2.66	–3.52	766.8078	Q11fe	11110	1	0	00010	1	0		
261	8470.5693	0.9688E–26	8470.5694	–0.08	–0.04	858.4393	Q14fe	11110	1	0	00010	1	0		
261	8470.1771	0.2393E–25	8470.1782	–1.07	–1.76	893.6768	Q15fe	11110	1	0	00010	1	0		

To be more specific the parameters of 69 from 93 lines were replaced by the data of ref. [10] in the $\nu_1+\nu_3+\nu_4$ band, 90 from 131 in the $\nu_1+\nu_3+\nu_4+\nu_5^1-\nu_5^1$ band, 103 from 170 in the $\nu_1+\nu_3+\nu_4+\nu_4^1-\nu_4^1$ band, 50 from 74 in the $\nu_1+2\nu_2+(\nu_4+\nu_5)^0$ band, 11 from 67 in the $2\nu_1+(2\nu_4+\nu_5)^1$I band, 39 from 126 in the $2\nu_1+\nu_2+\nu_4^1-\nu_5^1$ band, 29 from 55 in the $3\nu_2+(\nu_4+3\nu_5)^0$ band and 32 from 63 in the $\nu_1+\nu_3+\nu_4$ band of $^{13}C^{12}CH_2$. This information is included in the supmat1 and we believe that it does not deserve to be given in the text.

Data from HITRAN16 or from Vander Auwera et al. Mol Phys 2002;100:3563-76 + Jacquemart et al, JQSRT 2009 ;110 ;732-742 were NOT used in the fits.

- In Fig 10, a comparison between experimental spectrum and synthetic spectrum (calculated absorption coefficients) based on recommended line list will be more judicious, with obs - calc residuals. This will allow to really see how the recommended line list is matching with experimental spectrum. By plotting the recommended intensities versus experimental spectrum, you compare oranges and apples. I understood such plots for Fig 3 and 4 because it gives global information concerning how is ASD compares to this work in the view of the experimental spectrum, but for Fig 10, you compare in a final plot the exp spectrum and the recommended line list. Why not using calculated absorption coefficients based on recommended line list to compare oranges with observed absorption coefficients ?

It seems that the reviewer is distorting the contents of our paper to criticize it. His/her remarks would be appropriate if we were claiming that this Fig. 10 illustrates the agreement between the observed spectrum and that simulated from our recommended list. This is not the case. The purpose of this figure is to show that interpolation procedure allows to complement line list by lines which are important but hard to obtain from the spectra fitting. This is why the text introducing Fig.10 is the following: "*The superposition of the experimental spectrum to the recommended list presented in* ***Fig. 10*** *shows a number of calculated lines near the head of the Q-branch of the* $2\nu_3+(2\nu_4+\nu_5)^1$*I band at 8398.7* cm^{-1} *which cannot be derived experimentally but are included in the recommended list. "* and the caption of Fig. 10 is the following:

Fig. 10

Comparison of the CRDS spectrum of acetylene (P= 10 Torr) to the obtained recommended empirical line list (red stars). Note the calculated lines near the head of the Q-branch of the $2\nu_3+(2\nu_4+\nu_5)^1$I band near 8399 cm^{-1} and the presence of unassigned lines.

We thank the two reviewers and hope that the amended version is now suitable for publication in JQSRT.

Highlights

- A high sensitivity absorption spectrum of acetylene is recorded by CRDS near 1.2 μm
- More than 2600 lines are assigned to a total of 52 bands of $^{12}C_2H_2$, $^{12}C^{13}CH_2$ and $^{12}C_2HD$
- Spectroscopic parameters and Herman-Wallis coefficients are derived
- Comparison to literature data is discussed
- A recommended empirical line list is provided for the 8210-8670 cm^{-1} region

Graphical Abstract

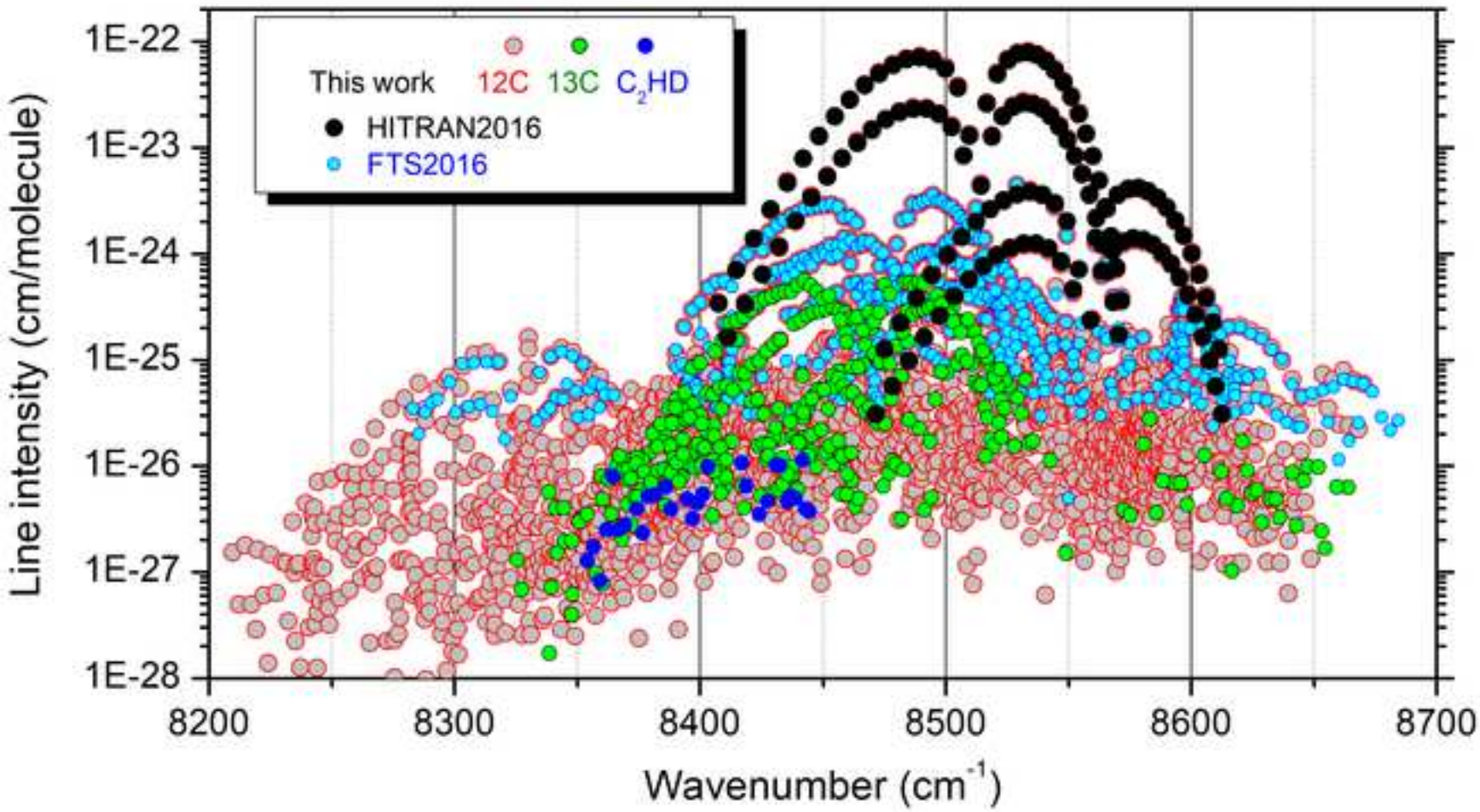

High sensitivity absorption spectroscopy of acetylene near 1.2 µm

O. M. Lyulin [1], S. Kassi [2] and A. Campargue [2*]

[1] *Laboratory of Theoretical Spectroscopy, V.E. Zuev Institute of Atmospheric Optics SB RAS, 1, Academician Zuev square, Tomsk 634055, Russia*
[2] *Univ. Grenoble Alpes, CNRS, LIPhy, 38000 Grenoble, France*

Number of Figures: 10
Number of Tables: 3

Running Head: *CRDS of acetylene near 8300 cm^{-1}*

Keywords: *acetylene; C_2H_2; effective Hamiltonian; CRDS; spectroscopic database; HITRAN*

* Corresponding author
E-mail: alain.campargue@univ-grenoble-alpes.fr
Tel: +33 4 76 51 43 19

Friday, May 7, 2021

ABSTRACT

The weak high-resolution absorption spectrum of natural acetylene has been recorded by high sensitivity cavity ring down spectroscopy (CRDS) near 1.2 μm. The frequency scale of the spectra was obtained by coupling the CRDS spectrometer to a self-referenced frequency comb. The room temperature recordings, performed at a pressure of 10.0 Torr, cover the 8210-8670 cm^{-1} spectral interval. A list of more than 11000 lines was constructed in the region. The smallest intensity values are on the order of 10^{-29} cm/molecule which is more than two orders of magnitude smaller than previous measurements by Fourier transform spectroscopy (FTS). More than 2600 lines were rovibrationally assigned using previous observations and predictions based on the effective operator approach. They include 2270, 338 and 28 absorption lines of $^{12}C_2H_2$, $^{12}C^{13}CH_2$ and $^{12}C_2HD$, respectively, belonging to a total of 52 vibrational bands, thirty-six of them being newly reported. For comparison, the HITRAN2016 database provides line parameters of only two $^{12}C_2H_2$ bands in the same region. Spectroscopic parameters of the upper vibrational levels were derived from standard band-by-band fits of the line positions (typical *rms* values of the (obs.-calc.) deviations are better than 0.002 cm^{-1}). The vibrational transition dipole moment squared and Herman-Wallis coefficients of 39 bands were derived from a fit of the intensity values measured in this work combined with previous FTS data for the strongest bands. A recommended list is constructed in the region using calculated line parameters for the unperturbed bands and experimental positions and intensities for the others. The recommended list including a total of 3139 transitions will help to complete acetylene spectroscopic databases in the near-infrared.

1. Introduction

During the recent years, we have undertaken a systematic experimental study of the high sensitivity acetylene absorption spectrum at room temperature in order to elaborate an empirical line list in the near infrared. Indeed, up to their HITRAN2016 [1] and GEISA2015 [2] editions, these spectroscopic databases provided only a few strong (mostly isolated) bands while the acetylene spectrum is much richer (see **Fig. 1**). A high number of additional bands were reported in the literature (see for instance Refs. [3-8]) but, in absence of intensity information, they could not be incorporated in spectroscopy databases.

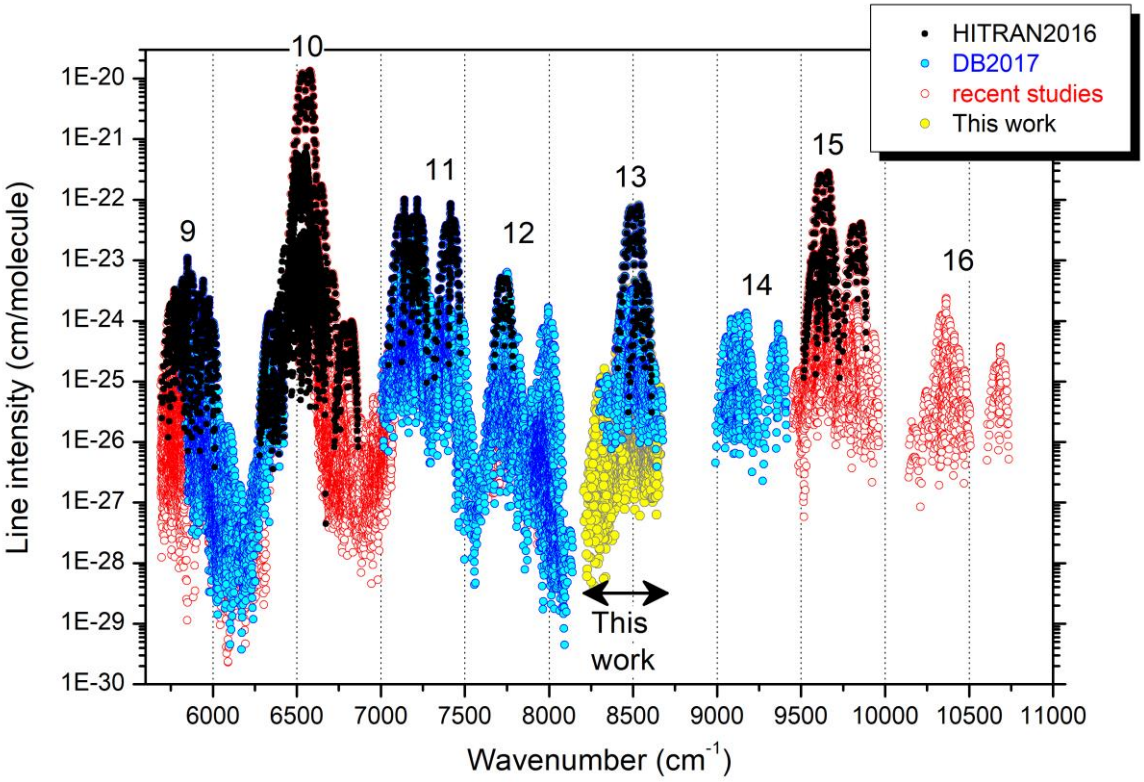

Fig. 1
Overview of the acetylene spectrum between 5600 and 11000 cm^{-1}. The HITRAN2016 linelist [1] (full black circles) is superimposed to our DB2017 empirical list [15] (blue circles) and to recent CRDS and FTS works [16-18, 21] (red circles). The present study in the 8210-8670 cm^{-1} spectral interval corresponds to the yellow circles. The ΔP values are indicated.

As illustrated in **Fig. 1**, the considered 5680-11000 cm^{-1} spectral interval includes strong absorption bands and regions of very low absorption (the acetylene transparency "windows"). As a result, lines with intensities spanning ten orders of magnitude have been measured by different techniques. Our analysis used spectra recorded by Fourier-transform spectroscopy (FTS) in the region of the strong bands and by cavity ring down spectroscopy (CRDS) in the weak absorption intervals. In 2017, by gathering the results of three FTS [9-11] and three CRDS [12-14] studies, we constructed a first version of our spectroscopic database (DB2017, hereafter) covering the 5850-9415 cm^{-1} region

(excluding the 6341-7000 cm^{-1} interval) [15]. As a rule, the DB2017 list relies on a band-by-band modeling: the acetylene line positions were calculated using empirical spectroscopic parameters of the lower and upper energy vibrational levels and intensities were computed using the vibrational transition dipole moment squared and Herman-Wallis coefficients derived, for each band, from a fit of measured intensities. This band-by-band approach allowed completing the experimental list by adding missing lines and improving poorly determined positions and intensities. In the case of perturbations, when part of the line parameters cannot be reproduced with an isolated band model, experimental line centers and line intensities were preferred. Compared to the HITRAN2016 [1] and GEISA2015 [2], the DB2017 list includes about ten times more bands and transitions.

The DB2017 list (5850-9415 cm^{-1}) was recently extended to lower and higher frequencies using CRDS spectra in the 5693-5882 cm^{-1} region [16] and FTS spectra in the 9280-10740 cm^{-1} interval [17,18], respectively. The resulting combined list covering the 5693-10740 cm^{-1} has been incorporated into the 2020 version of the HITRAN [19] and GEISA [20] databases.

Note that very recently, the 6627-7065 cm^{-1} transparency window was studied by CRDS [21]. This study, including a systematic derivation of line intensities, extended and completed previous studies limited to line positions and rovibrational assignments [7, 22].

In the present work, the 8200-8700 cm^{-1} region is studied for the first time by CRDS. The high sensitivity of the CRDS recordings will allow lowering considerably the detectivity threshold of the FTS spectra [10] used for DB2017, in particular in the 8200-8400 cm^{-1} interval where the very weak acetylene absorption is practically unknown (see **Fig. 1**).

At this step, it is necessary to underline that the assignment of weak bands in high sensitivity acetylene spectra is a difficult task and that a large fraction of lines (usually, more than 50%) remains unassigned in the CRDS spectra we recorded. Indeed, as a result of the achieved sensitivity (down to 10^{-29} cm/molecule), CRDS spectra are highly congested due to the superposition of many weak or super weak bands (including many hot bands and $^{12}C^{13}CH_2$ bands). Contrary to the strong bands dominating the spectrum which are generally regular, weak bands are frequently perturbed in positions and intensities. In addition, as a rule, part of the rotational transitions of these weak bands is obscured by stronger lines which makes difficult the use of lower state combination difference (LSCD) relations for rovibrational assignments. The assignment of our spectra relies greatly on the predictions of a global effective model developed at IAO-Tomsk for $^{12}C_2H_2$ [8]. This global model was used to generate the Acetylene Spectroscopic Databank (ASD) [23]. The ASD line positions are calculated using a global effective Hamiltonian (EH) with parameters values fitted against measured line positions available in the literature. The developed EH is a polyad model resulting from approximate relations between the acetylene normal mode harmonic frequencies. A given vibrational level is interacting through anharmonic and Coriolis interactions, with a limited set of vibrational levels, gathered in the so-called "vibrational polyads". Each polyad is characterized by the quantum number, $P= 5V_1+3V_2+5V_3+V_4+V_5$ where $V_{i=1-5}$ are the vibrational quantum numbers. Interpolyad interactions are not explicitly involved

but reproduced in an effective way by the fitted Hamiltonian parameters. A selection of about 25000 measured line positions in the 50-9900 cm^{-1} region was used to refine 237 EH parameters [8]. Using the resulting EH eigenfunctions, the effective dipole moment (EDM) parameters were fitted to measured intensity values for the ΔP = 0-13, 15 band series and used to compute the ASD line intensities in the 3-10000 cm^{-1} region [23] (the ΔP values are indicated on **Fig. 1**). Even if the ASD intensity cut-off (10^{-27} cm/molecule) is significantly higher than the CRDS detectivity threshold, the ASD line list includes a considerable number of calculated bands left to be observed. Although approximate (see below), these predictions are highly valuable to assign new spectra. In turn, new observations and new assignments are expected to help for future improvements of the global effective operator model.

The rest of the report is organized as follows. The experimental conditions and line parameters retrieval are presented in Section 2. Section 3 is devoted to the assignment procedure and comparison with ASD while the band-by-band analysis is presented in Sections 4 and 5, before the elaboration of the recommended line list (Section 6) and concluding remarks (Section 7).

2. Experimental details and line list construction

The CRDS spectra under analysis were recorded using an external cavity diode laser (ECDL) as light source. The reader is referred to Refs. [24-27] for the description of the cavity ring down spectrometer and the frequency tuning of the ECDL. The accurate frequency value associated to each ring-down event was obtained by using a Fizeau type wavemeter (High Finesse WS-U-30 IR) and a self-referenced frequency comb, providing sub-100 kHz accuracy to the instantaneous frequency readings [26, 28]. Mode-hop-free tuning range of up to 1.3 cm^{-1} could be obtained (see Ref. [26] for details). The broadband spectra covering the 8210-8670 cm^{-1} range was obtained by concatenation of a series of partly overlapping, 1.1 cm^{-1} wide individual spectra, recorded with about 1.3×10^{-3} cm^{-1} step sampling. Each baseline point was obtained by averaging 40 individual events. The spectra were recorded in flow regime in order to decrease the impact of the lines of water vapor degassing from the cell walls. The flow of acetylene (Air Liquide AAS27 99.7% stated purity) in natural isotopic abundance, was roughly adjusted to 1 sccm with a downstream manual needle valve and the pressure was actively regulated at 10.00 Torr. Nevertheless, a number of interfering lines of water vapor (with relative concentration of about 0.1 %) were identified in the high energy part of the spectrum. In addition, methane, present as an impurity in the used acetylene sample was found to contribute significantly to the observed spectrum (see below). The temperature of the outer wall of the stainless steel gas cell was monitored with a PT 1000 resistive probe. Over the whole spectrum recordings, the temperature evolved in the 293.2 – 295.0 K range. **Fig. 2** illustrates the sensitivity and high dynamical range on the intensity scale. The noise equivalent absorption evaluated as the *rms* of the baseline fluctuations is lower than 1×10^{-11} cm^{-1}. As illustrated in **Fig. 2**, the spectral congestion, and not the quality of the spectrum, is the main limitation of the spectral analysis.

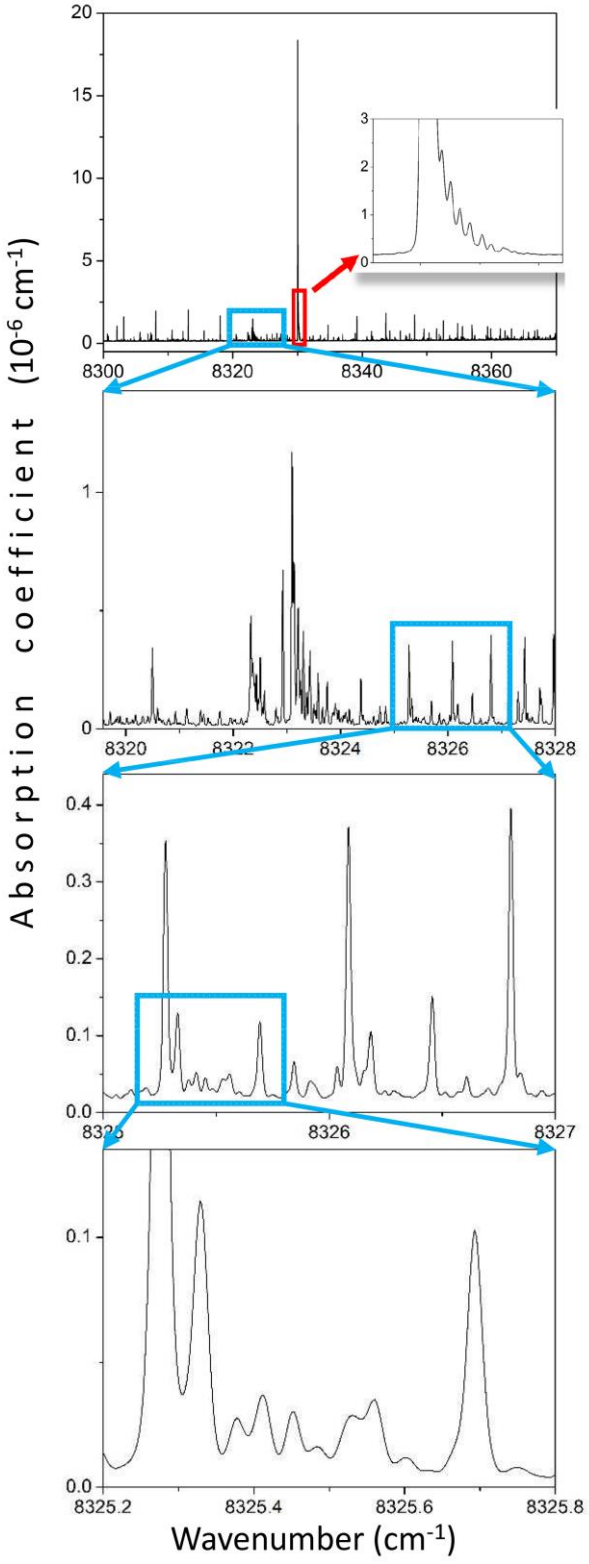

Fig. 2
CRDS spectrum of acetylene near 8330 cm^{-1} dominated by the strong *Q* branch of the $\nu_1+\nu_3+3\nu_4^1$ band. The sample pressure was 10 Torr. The superposition of the *Q* lines (see inset) leads to an unusually high absorption peak in the *Q* branch compared to the P and R lines. On the second panel, the *Q* branches of the $\nu_1+\nu_3+4\nu_4^2-\nu_4^1$ and $\nu_1+\nu_3+4\nu_4^0-\nu_4^1$ bands are observed near 8323 cm^{-1}. The strong regular lines on the third panel belong to the *Q* branch of the $\nu_1+\nu_3+3\nu_4^3$ forbidden band. The successive enlargements illustrate the high dynamics of the recordings and high congestion of the spectrum.

A homemade multiline fitting computer code was used to derive the line positions and intensities. The line shape was modeled with the Voigt profile with Gaussian width calculated for $^{12}C_2H_2$ Doppler broadening. The Doppler half width at half maximum of the line shape (HWHM) is about 0.01 cm^{-1} while the average pressure self-broadening of 0.14 cm^{-1}/atm [1] leads to a small Lorentzian contribution of about 2×10^{-3} cm^{-1}. The spectrum is very dense so the accuracy of the reported intensities depends on the weakness and overlapping of the considered lines. In the case of isolated lines with intensity larger than 10^{-27} cm/molecule, a 5% value is a conservative estimate of the uncertainty on the line intensity. Overall, line positions and intensities were derived for a total of more than 11500 lines. Using the HITRAN2016 database, about 200 and 3500 lines of water and methane lines (with relative concentrations of about 0.1 % and 0.2%, respectively) were removed from the line list. No other lines due to impurities were found in the spectrum, leaving about 8000 lines to be assigned in the 8202-8670 cm^{-1} region.

The derived dataset includes a few hundreds of very strong lines (with intensity up to 1×10^{-22} cm/molecule - see **Fig. 1**) while the weakest lines have an intensity on the order of 1×10^{-29} cm/molecule, seven orders of magnitude smaller. Accurate line parameters could not be derived for the strongest lines which appear "saturated" in the recorded CRDS spectra, because their large absorption drastically reduces the light intensity transmitted by the high-finesse CRDS cell. Consequently, we adopted for about 420 lines with intensity larger than 1×10^{-25} cm/molecule, the FTS line parameters of Ref. [10] obtained at a pressure of 42.4 Torr and an absorption pathlength of 48.3 m. The FTS source of the line parameters is indicated in the line list provided in the Supplementary Material I.

3. Rovibrational assignments

In a first step, the assignments available in the literature were transferred to our list:

(i) about 630 strong $^{12}C_2H_2$ lines have been assigned in our previous FTS study [10],

(ii) lines due to the $^{12}C^{13}CH_2$ isotopologue, present in natural isotopic abundance in the sample (about 2.2 %), were assigned on the basis of the line positions reported by Di Lonardo et al. [29], from FTS spectra recorded with a sample highly enriched in $^{12}C^{13}CH_2$. A total of 338 lines of seven vibrational bands were collected,

(iii) Finally, using the exhaustive review and line parameters published by Liévin et al. [30], twenty-eight lines of the $2\nu_1+\nu_2$ band of C_2HD could be identified. (The natural isotopic abundance of C_2HD in the sample is about 3×10^{-4}).

The assignment of the remaining observed lines of the main isotopologue was performed using the ASD-1000 calculated line list [23]. As mentioned above, this list was generated on the basis of the Tomsk effective Hamiltonian model developed in the frame of the effective operator approach [8] which considers all the resonance interactions between rovibrational levels up to the ninth order of perturbation theory. Despite of the facts that the CRDS spectrum is very dense and ASD line positions are sometimes significantly shifted compared to the observations (see **Figs. 3** and **4**), about 1650 $^{12}C_2H_2$ lines could be

newly assigned. It leads to a total of 2270 lines of 44 vibrational bands assigned for the main isotopologue, all belonging to the ΔP= 13 series. For comparison, the previous FTS study in the region provided 629 $^{12}C_2H_2$ lines of thirteen bands [10] and the HITRAN2016 database provides only the two strongest bands. It is worth giving the reader an idea of the difficulty of the assignment procedure relying on the comparison with the ASD calculated list. We provide in **Figs. 3** and **4** two examples of very different situations. In **Fig. 3,** only a limited fraction of the measured lines was assigned near 8324 cm^{-1} while there is a good visual coincidence between the recorded spectrum and the *Q* branches of $\nu_1+\nu_3+4\nu_4^2-\nu_4^1$ and $\nu_1+\nu_3+4\nu_4^0-\nu_4^1$ bands around 8323 cm^{-1} included in the ASD list. Unfortunately, both branches reverse their direction at some *J* value that considerable complicates the spectrum assignment. In such conditions the accuracy of the prediction is not sufficient for reliable assignments and in absence of lower state combination relations, the observed, relatively strong lines, remained unassigned. In **Fig. 4**, the ASD intensity of the *Q* branch of the band centered at 8378.2 cm^{-1} is predicted strongly overestimated (at least by a factor 20) which illustrates the difficulty to use the intensity agreement to assign new bands.

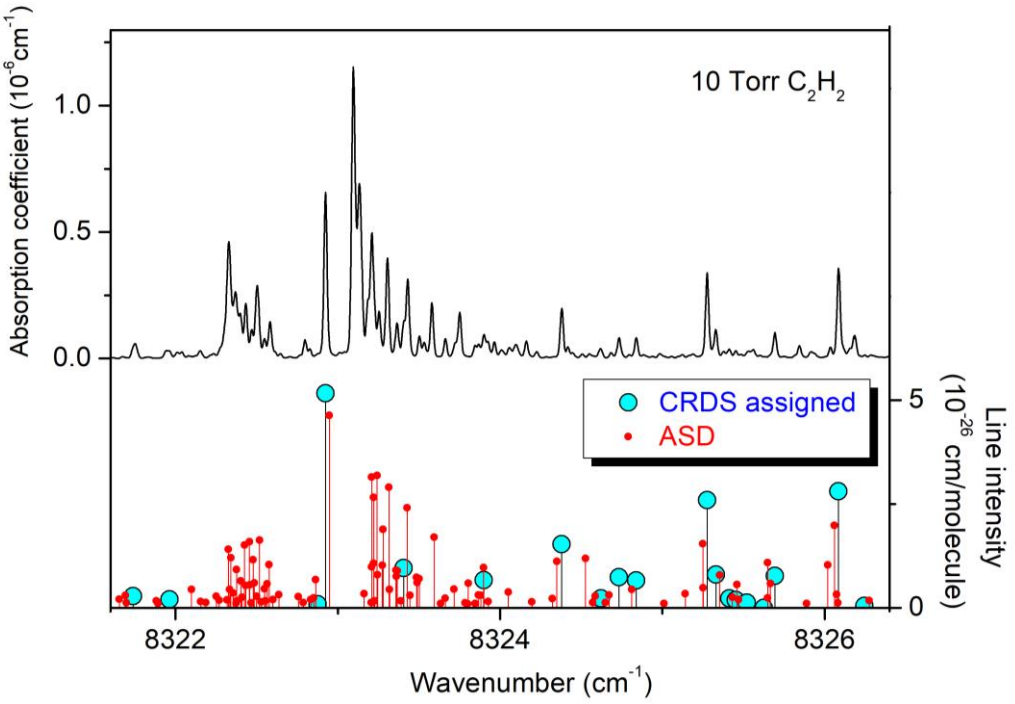

Fig. 3
Comparison of the CRDS spectrum of acetylene (*P*= 10 Torr) with the predicted spectrum provided by the Acetylene Spectroscopic Databank (ASD) [23] (red sticks). The stick spectrum with cyan circles correspond to the lines retrieved from the experimental spectrum which could be assigned. The visual coincidence between the experimental spectrum and the *Q* branches of the $\nu_1+\nu_3+4\nu_4^2-\nu_4^1$ and $\nu_1+\nu_3+4\nu_4^0-\nu_4^1$ bands provided by ASD around 8323 cm^{-1} was not sufficient to unambiguously assign the corresponding lines.

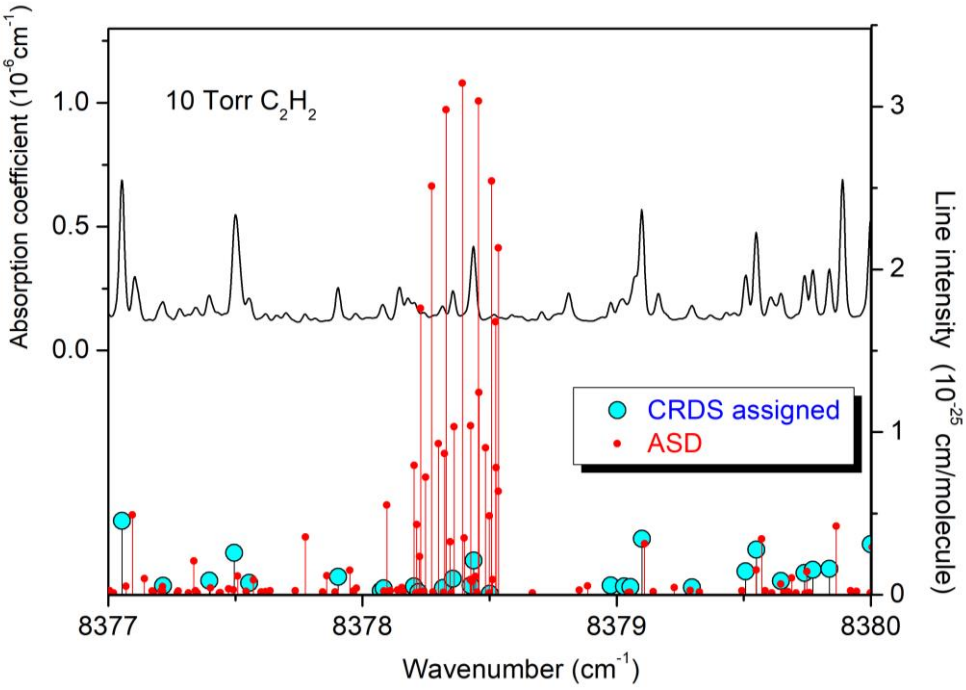

Fig. 4
Comparison of the CRDS spectrum of acetylene (*P*= 10 Torr) with the predicted spectrum provided by the Acetylene Spectroscopic Databank (ASD) [23] (red sticks) near 8378 cm^{-1}. The stick spectrum with cyan circles correspond to the lines retrieved from the experimental spectrum which could be assigned. The strong *Q* branch of a band centered at 8378.2 cm^{-1} included in the ASD list is not observed in the CRDS spectrum.

Overall, considering the three isotopologues, a total of 2636 lines of 52 vibrational bands could be assigned leaving a considerable number of lines without identification. The list of about 5000 unassigned lines is provided as Supplementary Material II. Although we cannot exclude that part of these unassigned lines are due impurities (*e.g.* ethylene), the majority of these lines are believed to be due to $^{12}C_2H_2$. An overview of our assigned list is presented in **Fig. 5** and compared to the HITRAN2016 list and to the previous FTS list of Ref. [10]. The weakest assigned lines have an intensity on the order of 10^{-28} cm/molecule, about two orders of magnitude below the FTS detectivity. Note that the HITRAN2016 includes only two bands and that the position and intensity comparisons between the FTS values of Ref. [10] and HITRAN2016 values were discussed in Ref. [10].

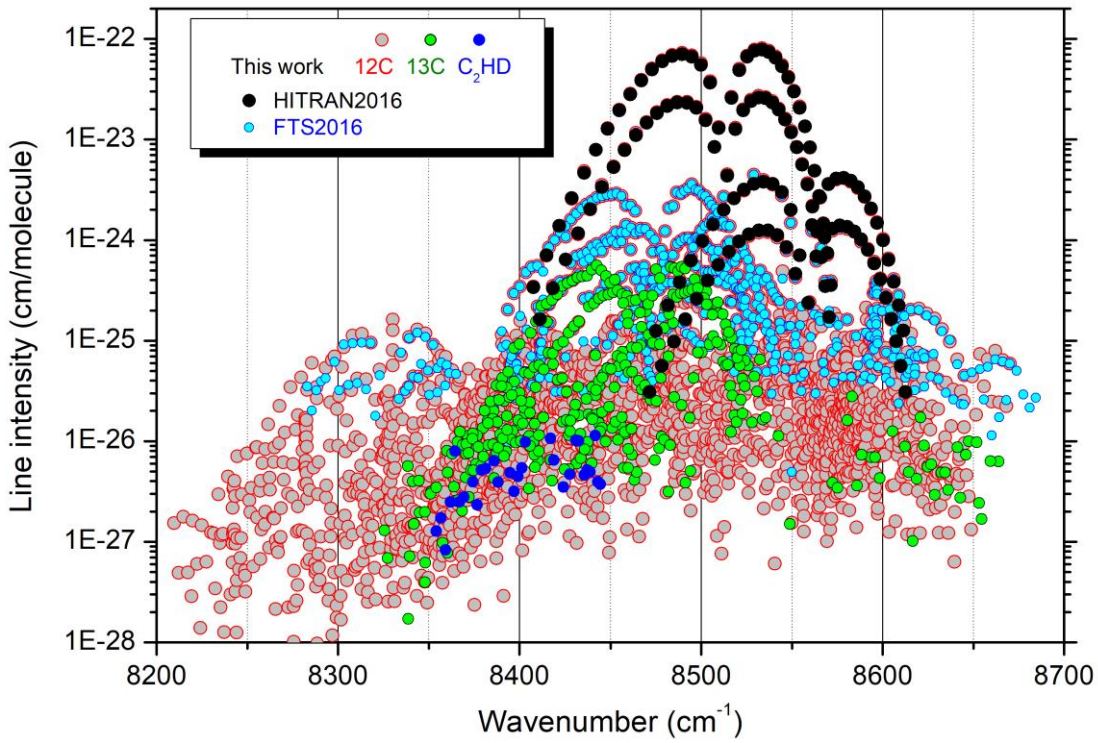

Fig. 5
Different line lists for acetylene in the 8200-8700 cm^{-1} region. The data from HITRAN2016 database [1] and the FTS measurements of Ref. [10] are plotted with black and light blue circles, respectively. The other symbols correspond to the $^{12}C_2H_2$, $^{12}C^{13}CH_2$ and $^{12}C_2HD$ absorption lines assigned in this work.

As illustrated in **Figs. 3** and **4**, for the assigned lines, the agreement between the measured and ASD positions is in general satisfactory. The results of the systematic position comparison presented in **Fig. 6**, indicate that most of the deviations are within 0.1 cm^{-1} except for two bands ($\nu_2+\nu_3+5\nu_4^1$ and $2\nu_2+(6\nu_4+\nu_5)^1$II near 8242 and 8282 cm^{-1}, respectively) where position differences up to 0.3 cm^{-1} are noted. These important deviations probably reveal the need to include some additional parameters in the effective Hamiltonian used for the generation of ASD. The evidenced deviations will be thus valuable to improve future versions of ASD. In general, deviations show a smooth *J* dependence for a given vibrational band. Note that this comparison might be biased by the fact that our assignments rely on the comparison with ASD and it might be that part of the lines left unassigned could not be identified because their measured positions deviate considerably compared to their ASD values.

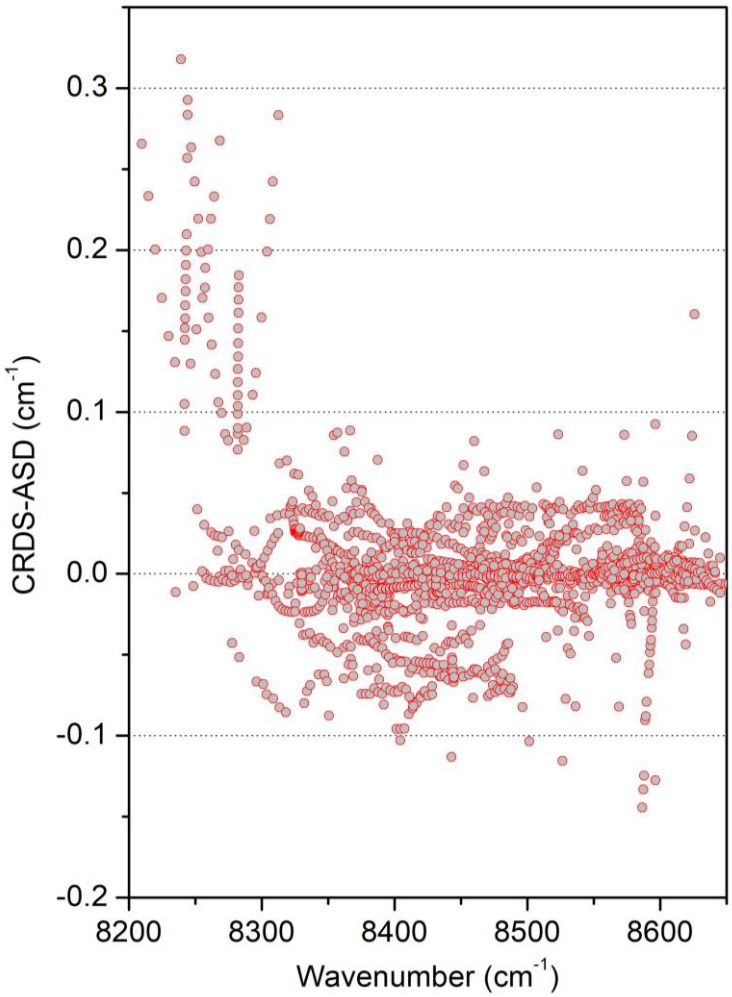

Fig. 6
Differences between the measured positions of $^{12}C_2H_2$ with corresponding calculated values included in the Acetylene Spectroscopic Databank [23] in the 8200-8670 cm^{-1} region.

The list of assigned lines is provided in the Supplementary Material I and includes the results of the fit of the spectroscopic parameters (see below). The assigned bands are listed in **Table 1**. In the first column, we provide for the upper vibrational state the ($v_1v_2v_3v_4v_5l_4l_5\varepsilon$) normal mode labeling and symmetry (*e* or *f*) of the Wang basic functions. The bands are ordered according to the upper energy value. The vibrational labeling is obtained from the global effective Hamiltonian [8] and usually corresponds to the maximum fraction of the low *J* eigenfunctions in the normal mode basis. We also give the band name in the vibrational notation of Plíva adopted in the HITRAN database: $v_1v_2v_3(v_4v_5)^{l\pm}r$ with $l=\left|l_4+l_5\right|$, l_t being the vibrational angular momentum quantum number associated with the degenerated bending mode t (t= 4,5), ± being the symmetry type for Σ vibrational states (l= 0), and r a roman numeral indicating the rank of the level, by decreasing energy value (r= *I* for the highest energy level), inside the set of states having the same l value. The letter "N" in the first column of **Table 1** marks newly observed upper vibrational levels. As one can see most of the upper levels were observed for the first time.

Thirteen bands of $^{12}C_2H_2$ and three bands of $^{13}C^{12}CH_2$ were observed in our previous FTS study in the region [10]. The present CRDS study allowed extending considerably the number of lines in the previously reported bands. For example, only several lines in the *Q* branches were observed by FTS for the $2\nu_3+(2\nu_4+\nu_5)^1$I, $2\nu_3+(2\nu_4+\nu_5)^1$II and $\nu_1+\nu_2+(4\nu_4+\nu_5)^1$II bands while, in this work, the *P* and *R* branches are presently assigned and the total number of measured lines is increased by a factor of five. Note that the band centered at 8515.62 cm^{-1}, presently labeled as $3\nu_2+(2\nu_4+3\nu_5)^1$III$-\nu_4^1$, was reported in DB17 [6] with another labeling of the upper vibrational level ($\nu_1+2\nu_2+(2\nu_4+\nu_5)^1I-\nu_4^1$). Indeed, the upper level of this band (G_v= 9127.31 cm^{-1}) belongs to the *P*= 14 polyad where three vibrational levels are in strong resonance interaction. The largest contribution to the upper level of the considered band gives ($v_1v_2v_3v_4v_5l_4l_5$) = (120212-1) but there is another energy level (G_v= 9142.997 cm^{-1}) having a greater contribution (about 50%) of this basic function. As a result, in the DB17 list, we have chosen the second largest contributor, 1202101, to label the upper state of this band. In the present work, we observed transitions to the three strongly interacting levels with energies at 9127.31, 9143.00 and 9152.80 cm^{-1}. The 120212-1 and 1202101 basic functions give contributions of about 50% to both the second and third vibrational levels. To avoid duplicate labeling, after an analysis of the interaction scheme, we decided to attribute the 030232-1 label (about 15% contribution) to the energy level at 9127.31 cm^{-1}.

4. Band by band analysis.

4.1. Spectroscopic parameters

The rotational analysis was performed using the standard formula for the rovibrational energy levels of an isolated vibrational state:

$$T(v, J, e/f) = G_{e/f} + B_{e/f}J(J+1) - D_{e/f}[J(J+1)]^2 + H_{e/f}[J(J+1)]^3 \quad (1)$$

where $G_{e/f}$ is the vibrational term value and $B_{e/f}$, $D_{e/f}$, and $H_{e/f}$ are the rotational and distortion constants of the *e* and *f* sub levels. The parameters of the lower vibrational levels of $^{12}C_2H_2$, $^{12}C^{13}CH_2$ and $^{12}C_2HD$ were constrained to their fitted values of Ref. [13], Ref. [31] and Ref. [30], respectively. As the *e* and *f* sub bands may be perturbed in a different way, different sets of spectroscopic parameters were fitted for the *e* and *f* levels. The retrieved constants of the upper states are listed in **Table 1**. The results of the fit are provided for each band in the Supplementary Material I. The bands reported in Refs. [10, 15] and the two bands of the HITRAN2016 database [1] are marked in the last column of the table by “Luy16”, “DB17” and “HIT16”, respectively.

Some of the studied bands were found to be affected by perturbations (they are marked with “P” in **Table 1**). **Fig. 7** illustrates an example of breaking of the regular rotational structure in the *Q* branch of the $2\nu_3+(2\nu_4+\nu_5)^1$II band near 8396 cm^{-1}. One can clearly observe that the positions of the *J*= 12,13 lines are shifted from their unperturbed positions. Perturbed positions were excluded from the fit. In the cases where the perturbation does not allow reproducing the rotational structure using Eq. (1), the levels with high rotational quantum number were generally excluded from input data, in order to achieve a reasonable fit for the lowest *J* values and thus a satisfactory determination of the vibrational term. This

was usually the case for the bands involving a double excitation of the ν_4 bending mode, in the lower or upper state.

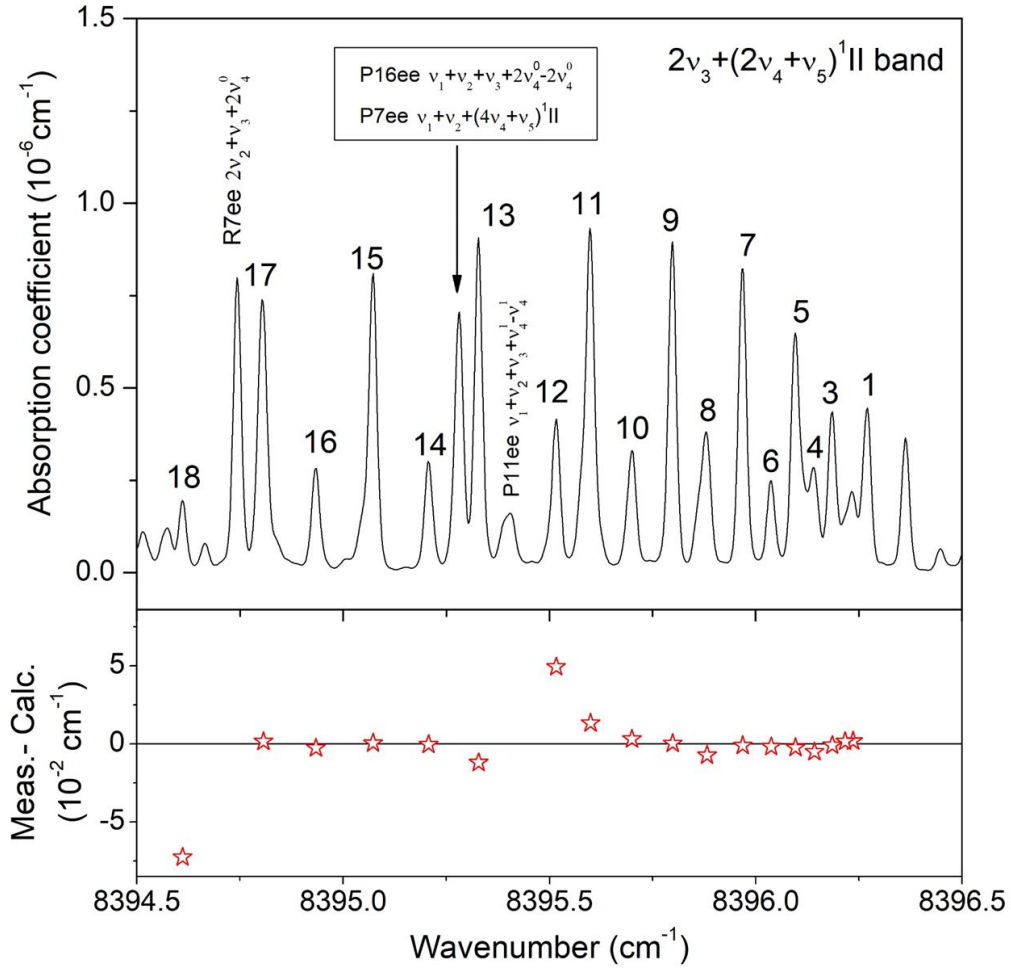

Fig. 7
Part of the *Q* branch of the $2\nu_3+(2\nu_4+\nu_5)^1$II band affected by a local perturbation for *J*= 12, 13. The corresponding lower *J* values are given. Four transitions belonging to other bands are also indicated. The lower panel shows the (meas.-calc) position residuals obtained from the fit of the upper state constants.

A similar situation was found for the $\nu_1+\nu_3+3\nu_4^1$ and $\nu_1+\nu_3+3\nu_4^3$ bands centered at 8330 cm^{-1} and 8329.3 cm^{-1}, respectively. The two principal contributions of the basic functions to the corresponding interacting upper states were obtained from the global effective modeling [8] and are plotted in **Fig. 8** as a function of the upper state angular moment quantum number. The obtained *J* dependence illustrates the large variation of the eigenfunctions composition with the *J* value. The distortion constants of the perturbed bands are usually anomalously large or negative. After exclusion of the lines with poorly determined centers or affected by perturbation, the average *rms* values of the (meas.- fit) differences are on the order of 1.5×10^{-3} cm^{-1} which is close to our claimed accuracy on the measured line positions.

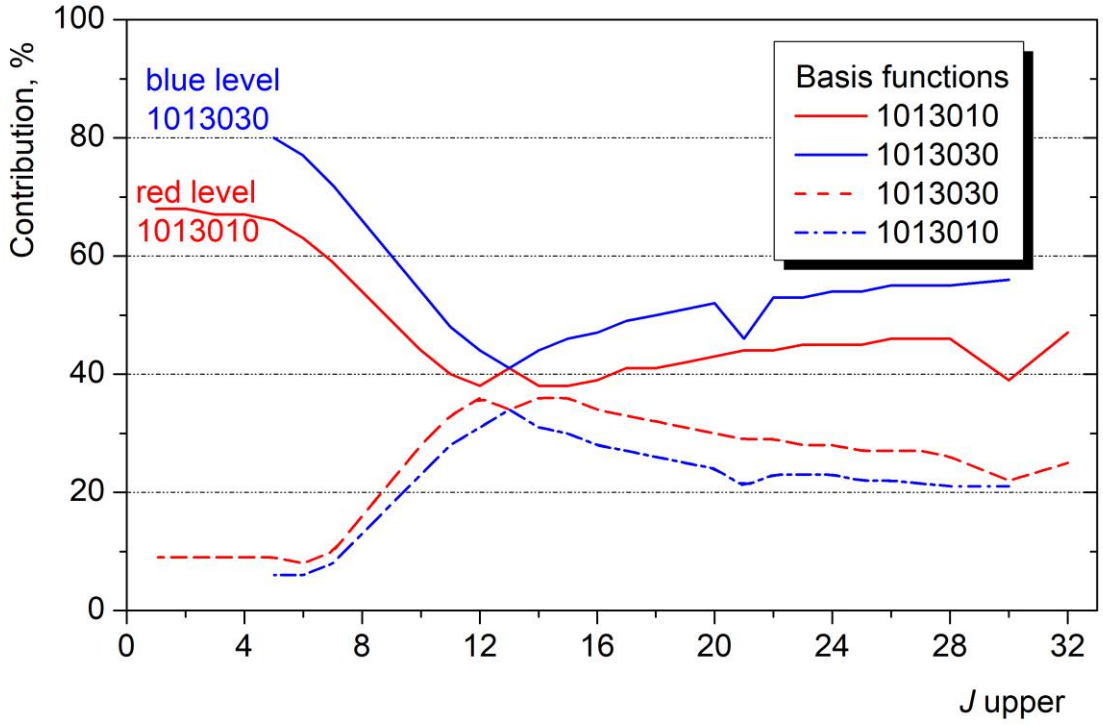

Fig. 8

Interaction between 1013030e and 1013010e vibrational levels. The first and second basic function contributions are plotted by solid and dashed lines, respectively while the blue and red colors correspond to the levels labeled 1013030e and 1013010e, respectively.

5. Line intensities

According to the isolated band model, the intensity of an absorption transition between the $V'J'\varepsilon'$ and $VJ\varepsilon$ states (V and J are the vibrational index and the angular momentum quantum number, respectively, and ε= ± is the parity) at a temperature T (in K) is related to the transition dipole moment squared $|R|^2$:

$$S_{V'J'\varepsilon'\leftarrow VJ\varepsilon}(T) = \frac{8\pi^3}{3hc} C g_{VJ\varepsilon} \frac{\nu_{V'J'\varepsilon'\leftarrow VJ\varepsilon}}{Q(T)} exp\left(-\frac{hcE_{VJ\varepsilon}}{kT}\right)\left[1-exp\left(-\frac{hc\nu_{V'J'\varepsilon'\leftarrow VJ\varepsilon}}{kT}\right)\right] L(J,K)|R|^2 \qquad (2)$$

where $E_{VJ\varepsilon}$ is the lower state energy and $\nu_{V'J'\varepsilon'\leftarrow VJ\varepsilon}$ is the transition wavenumber, $Q(T)$ is the total internal partition function at temperature T, C is the isotopic abundance, $g_{VJ\varepsilon}$ is the nuclear statistical weight of the lower state and $L(J,K)$ is Hönl-London factor. The values of the total internal partition functions of $^{12}C_2H_2$, $^{12}C^{13}CH_2$ and C_2HD, and their natural isotopic abundances were taken from the HITRAN2016 [1].

The expression of the Hönl-London factors for parallel (ΔK= 0), perpendicular (ΔK = ±1) and ΔK = ±2 forbidden bands can be found in Ref. [15], and in Ref. [32] for ΔK = ±3. However $L(J,K)$ calculations for $|\Delta K|>1$ have been performed here using more common recurrent expression:

$$L^{\Delta K}(J,K) = L^{\Delta K-s}(J,K+s)\left(J\left(J+1\right)-K\left(K+s\right)\right) \qquad (3)$$

where $L^{\Delta K}(J,K)$ is the Hönl-London factor for any $|\Delta K|>1$, and "s" depends on the sign of ΔK: $s = +1$ and -1 for positive and negative values of ΔK, respectively.

The rotational dependence of the transition moment squared $|R|^2$ is taken into account using Herman-Wallis coefficients A_1^{RP}, A_2^{RP}, and A_2^{Q}:

$$|R|^2 = |R_0|^2 (1 + A_1^{RP} m + A_2^{RP} m^2)^2 \text{ (}P\text{- and }R\text{-branches)}, \quad (4)$$

$$|R|^2 = |R_0|^2 (1 + A_2^{Q} m^2)^2 \text{ (}Q\text{-branch)}, \quad (5)$$

m being equal to $-J$ in the P-branch, J+1 in the R-branch, and J in the Q-branch and $|R_0|^2$ is the vibrational transition dipole moment squared. Note that we use the squared form of the terms between parentheses in Eqs. (4,5) accordingly to our previous publication [15].

Vibrational transition dipole moments squared and Herman-Wallis coefficients obtained from an unweighted fit of the experimental intensity values are reported in **Table 2**. As a combined effect of perturbations and experimental uncertainties due to line overlapping and to the weakness of many bands, a significant number of line intensities had to be excluded from the fit. Even with a reduced input dataset, a satisfactory fit could not be achieved for a significant number of bands. In such cases, we provide only the vibrational transition moment squared value with a large uncertainty. The root mean square deviation of the intensity fit given by the fitting procedure is included in **Table 2** and is about 7%. In many cases, in view of the number of intensity values which were excluded, it seems that the obtained *rms* values overestimate the quality of the fits and we give in the last column of **Table 2** our own estimation of the relative error bars of the intensities calculated with the obtained set of parameters.

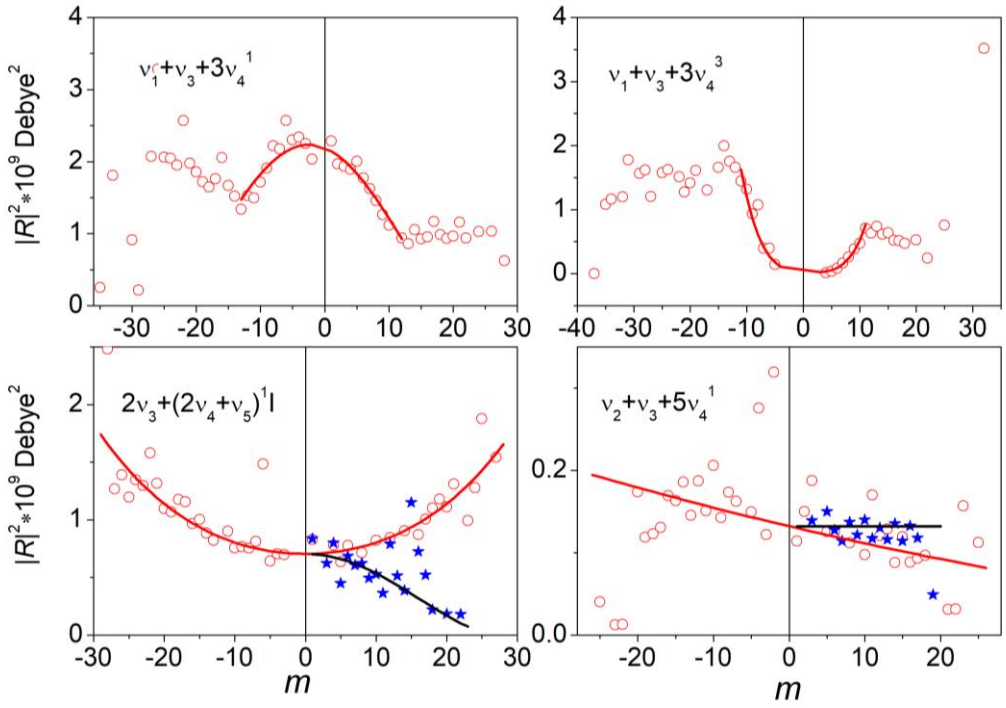

Fig. 9
Four examples of the line intensity fits of the different cold bands (see details in the text). Red circles correspond to $|R|^2$ values of the P and R branches, while blue stars correspond to the Q branch. (m stands

for $-J$, J, $J+1$ for P, Q, R branches, respectively). The solid lines correspond to the fitted values of $|R_0|^2$ and Herman-Wallis factors.

Most of the bands assigned in the region show a weak rotational dependence of transition dipole moment squared. Four examples of rotational dependence are presented in **Fig. 9**. The two upper panels are related to the $\nu_1+\nu_3+3\nu_4^1$ and $\nu_1+\nu_3+3\nu_4^3$ interacting bands presented in **Fig. 8**. This is a typical example where the interaction prevents a polynomial fit of the transition dipole moments of the interacting bands. The two other examples, presented in the lower part of the figure, show weak rotational dependence and typical scattering of the measured values.

6. Recommended empirical line list

Following the procedure adopted to construct the DB17 acetylene list [15], we elaborated a list recommended for the studied region which is provided as Supplementary Material III. On the basic of the empirical parameters obtained from the measured positions and intensities, a line list was generated for each band listed in **Table 2** at the reference temperature of 296 K. For each branch of a given band, line parameters were calculated for all the transitions up to a maximum J value generally exceeding by 1 the largest J value included into the intensity fit. Line positions were computed using the spectroscopic constants of **Table 1** and line intensities were obtained from $|R_0|^2$ and Herman-Wallis factors collected in **Table 2**. This approach allows averaging the measurement errors, completing the experimental observations by interpolation between measured lines and slightly extending the list beyond the observations. This is especially important in the highly congested Q-branch region as well as in the case of weak bands, where a significant number of lines are obscured by stronger ones. The superposition of the experimental spectrum to the recommended list presented in **Fig. 10** shows a number of calculated lines near the head of the Q-branch of the $2\nu_3+(2\nu_4+\nu_5)^1$I band at 8398.7 cm^{-1} which cannot be derived experimentally but are included in the recommended list. Note the presence of a few unassigned lines with intensity on the order of 10^{-26} cm/molecule, in the displayed spectral interval.

The studied region is the highest frequency region that we investigated by CRDS. As a result of the sensitivity of the recordings and of the high energy range, perturbations are frequent and the band-by-band model is often insufficient to account for the observations. As a rule, the direct comparison to the spectrum was used to make to best choice between the measured and calculated line parameters. In general, calculated values were kept if the band intensity fit was successful and no perturbation was noticed around the considered line. When the calculated line position was found clearly shifted from the observed line center, we kept the measured value and marked such lines with a “p” tag in the Supplementary Material III. No interpolation or extrapolation was performed around perturbed J values. In the cases where the intensity fit failed or the measured intensity was significantly smaller than the calculated value, the measured value was transferred to the recommended line list with a “e” tag. The recommended line list contains 2707 lines of $^{12}C_2H_2$, 404 lines of $^{13}C^{12}CH_2$ and 28 lines of $^{12}C_2HD$. The number of lines is given for every band in sixth column of **Table 2**.

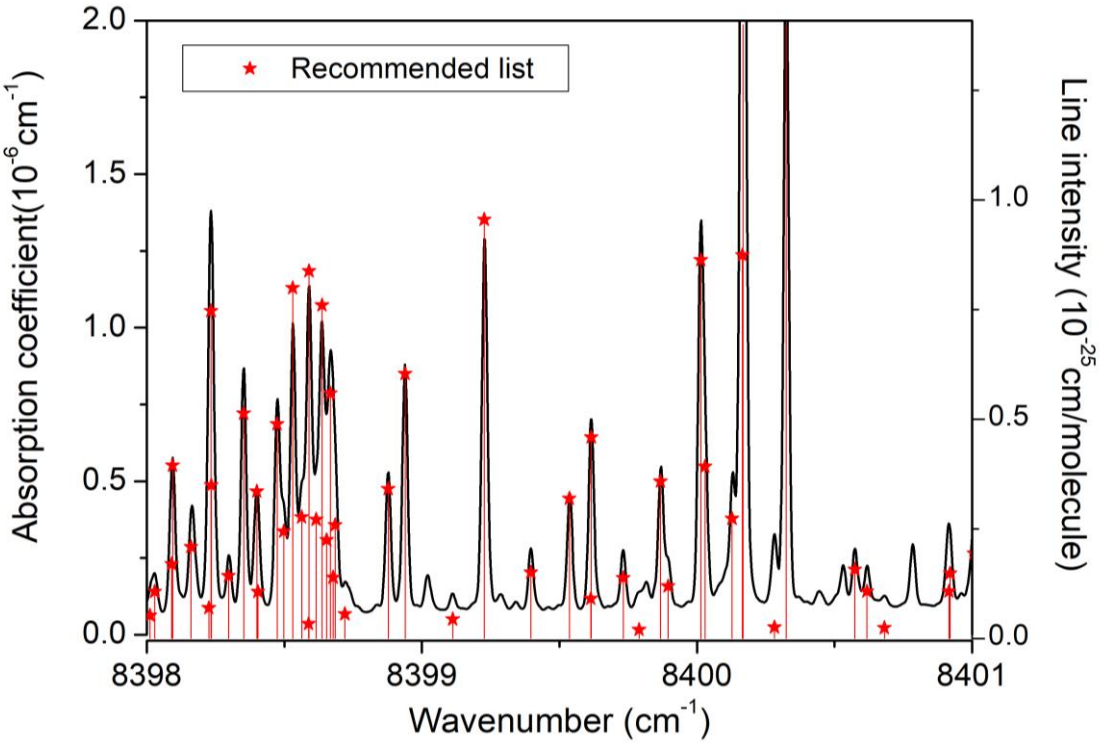

Fig. 10
Comparison of the CRDS spectrum of acetylene (P= 10 Torr) to the obtained recommended empirical line list (red stars). Note the calculated lines near the head of the Q-branch of the $2\nu_3+(2\nu_4+\nu_5)^1$I band near 8399 cm^{-1} and the presence of unassigned lines.

7. Concluding remarks

The high-resolution CRDS absorption spectrum of acetylene has been recorded with unprecedented sensitivity in the 1.2 μm region (8210-8670 cm^{-1}) corresponding to a ΔP= 13 variation of the polyad quantum number. The predictions of the global effective operator model developed at IAO-Tomsk [10] as provided in the ASD list [23] have allowed assigning new bands and extending the assignments of already known bands. Nevertheless, besides the usual shift between predicted and measured positions of newly observed lines, significant issues concerning line intensities were evidenced (see *e. g.* **Fig. 5**).

Table 3
Statistical comparison of the number of lines and bands obtained in this work, provided by the HITRAN database [1] or reported in the previous FTS study [15] in the 8200-8700 cm^{-1} spectral interval.

	$^{12}C_2H_2$		$^{12}C^{13}CH_2$		$^{12}C_2HD$	
	Band	Line	Band	Line	Band	Line
HITRAN2016 [1]	2	131				
FTS [10]	13	629	3	114		
Measured/Recommended	44	2270[a]/2707	7	338/404	1	28/28

Note
[a] Including 421 (strong) lines transferred from Ref. [10].

The statistical comparison of the amount of data provided by the HITRAN2016 database [1], obtained from a previous FTS study in the region [10] and in the present work is presented in **Table 3**. Our recommended list based on a band-by-band modeling of the assigned lines includes a total of about 3100 transitions of 52 bands of the $^{12}C_2H_2$, $^{12}C^{13}CH_2$ and $^{12}C_2HD$ isotopologues present in natural isotopic abundance in our sample. Thirty-six of these bands are newly reported. It is worth underlying that our observations include many hot bands with upper levels belonging to higher energy polyads (up to P= 16 above 10000 cm^{-1}) for which neither the band-by-band approach nor the global effective operator approach is fully satisfactory. This is the reason why a significant number of experimental line positions and line intensities were kept in our recommended list of assigned transitions in the region. As a further illustration of the limits of our knowledge of the near infrared absorption spectrum of acetylene, let us recall that about 5000 mostly weak lines measured in this work remain unassigned. They are provided as supplementary material for future assignments or tests of theoretical calculations of the acetylene spectrum based on the improvement of the effective operator approach or variational calculations.

Acknowledgements

This work is supported by CNRS (France) in the frame of the International Research Project "SAMIA" with IAO-Tomsk. O.L thanks Université Grenoble Alpes for a two-months support at LIPhy Grenoble. The analysis was supported by the Ministry of Science and Higher Education of the Russian Federation (V.E. Zuev Institute of Atmospheric Optics of Siberian Branch of the Russian Academy of Sciences).

References

1. Gordon IE, Rothman LS, Hill C, Kochanov RV, Tan Y, Bernath PF, et al. The HITRAN2016 molecular spectroscopic database. J Quant Spectrosc Radiat Transfer 2017;203:3–69. doi:10.1016/j.jqsrt.2017.06.038.
2. Jacquinet-Husson N, Armante R, Crépeau N, Chédin A, Scott NA, Boutammine C, et al. The 2015 edition of the GEISA spectroscopic database. J Mol Spectrosc 2016;327:31–72. doi:10.1016/j.jms.2016.06.007
3. Campargue A; Temsamani MA; Herman M. The absorption spectrum of C_2H_2 between 12800 and 18000 cm^{-1}: I. Vibrational assignments. Molecular Physics 1997;90:793–805.
4. Herman M, Liévin J, Vander Auwera J, Campargue C. Global and accurate vibration hamiltonians from high-resolution molecular spectroscopy. Adv Chem Phys 1999;108:1–431. Wiley, New York.
5. Herman M, Campargue C, El Idrissi MI, Vander Auwera J. Vibrational spectroscopic database on acetylene, $\widetilde{X}^1\Sigma_g^+$ ($^{12}C_2H_2$, $^{12}C_2D_2$ and $^{13}C_2H_2$) J Phys Chem Ref Data 2003;32:921–1361.
6. Fayt A, Robert S, Di Lonardo G, Fusina L, Tamassia F, Herman M. Vibration-rotation energy pattern in acetylene: $^{12}CH^{12}CH$ up to 6750 cm^{-1} J Chem Phys 2007;126:114303/1–8..
7. Amyay B, Herman M, Fayt A, Campargue A, Kassi S. Acetylene, $^{12}C_2H_2$: refined analysis of CRDS spectra around 1.52 µm. J Mol Spectrosc 2011;267:80–91.
8. Lyulin OM, Perevalov VI. Global modelling of vibration-rotation spectra of acetylene molecule. J Quant Spectrosc Radiat Transf 2016;177:59–74.
9. Lyulin OM, Vander Auwera J, Campargue A. The Fourier transform absorption spectrum of acetylene between 7000 and 7500 cm^{-1}. J Quant Spectrosc Radiat Transf 2015;160:85–93.
10. Lyulin OM, Vander Auwera J, Campargue A, The Fourier transform absorption spectrum of acetylene between 8280 and 8700 cm^{-1}. J Quant Spectrosc Radiat Transf 2016;177:234–240 http://dx.doi.org/10.1016/j.jqsrt.2015.11.026
11. Béguier S, Lyulin OM, Hu SM, Campargue A. Line intensity measurements for acetylene between 8980 and 9420 cm^{-1} J Quant Spectrosc Radiat Transf 2017;189:417-420. 10.1016/j.jqsrt.2016.12.020
12. Lyulin OM, Campargue A, Mondelain D, Kassi S. The absorption spectrum of acetylene by CRDS between 7244 and 7918 cm^{-1} J Quant Spectrosc Radiat Transf 2013;130:327–43.
13. Lyulin OM, Mondelain D, Béguier S, Kassi S, Vander Auwera J, Campargue A. High sensitivity absorption spectroscopy of acetylene by CRDS between 5851 and 6341 cm^{-1}. Mol Phys 2014;112:2433–44.
14. Kassi S, Lyulin OM, Béguier S, Campargue A. New assignments and a rare peculiarity in the high sensitivity CRDS spectrum of acetylene near 8000 cm^{-1}. J Mol Spectrosc 2016;326:106-114.
15. Lyulin OM, Campargue A. An empirical spectroscopic database for acetylene in the regions of 5850-6341 cm^{-1} and 7000-9415 cm^{-1}. J Quant Spectrosc Radiat Transf 2017;203:461–471. 10.1016/j.jqsrt.2017.01.036
16. Lyulin OM, Vasilchenko S, Mondelain D, Campargue A. The CRDS spectrum of acetylene near 1.73 µm J. Quant. Spectrosc. Radiat. Transfer 234 (2019) 147–158. doi.org/10.1016/j.jqsrt.2019.04.006
17. Lyulin OM, Béguier S, Hu SM, Campargue A, The absorption spectrum of acetylene near 1 µm (9280–10740 cm^{-1}) (I): Line positions. J Quant Spectrosc Radiat Transf 2018;208:179-187 DOI: 10.1016/j.jqsrt.2018.01.007
18. Lyulin OM, Campargue A. The absorption spectrum of acetylene near 1 µm (9280–10740 cm^{-1}) (II): Line intensities. J Quant Spectrosc Radiat Transf 2018;215:51-58. DOI: 10.1016/j.jqsrt.2018.04.025
19. Gordon IE, Rothman LS, et al. The HITRAN2020 molecular spectroscopic database. J Quant Spectrosc Radiat Transfer, submitted
20. Delahaye T, Armante R, Scott NA, et al. The 2020 edition of the GEISA spectroscopic database. J Mol Spectrosc, submitted
21. Lyulin OM, Vasilchenko S, Mondelain D, Kassi S, Campargue A. The acetylene spectrum in the 1.45 µm window (6627-7065 cm^{-1}). J. Quant. Spectrosc. Radiat. Transfer 253 (2020) 107057 doi.org/10.1016/j.jqsrt.2020.107057
22. Robert S, Herman M, Fayt A, Campargue A, Kassi S, Liu A, et al. Acetylene, $^{12}C_2H_2$: new CRDS data and global vibration-rotation analysis up to 8600 cm^{-1}. Mol Phys 2008;106:2581–605.
23. Lyulin OM, Perevalov VI. ASD-1000: High-resolution, high-temperature acetylene spectroscopic databank. J Quant Spectrosc Radiat Transf 2017;201:94–103.
24. Mondelain D, Kassi S, Sala T, Romanini D, Marangoni M, Campargue A. Sub-MHz accuracy measurement of the S(2) 2–0 transition frequency of D2 by comb-assisted cavity ring down spectroscopy. J Mol Spectrosc 2016;326:5–8. https://doi.org/10.1016/j.jms.2016.02.008.
25. Kassi S, Campargue A. Cavity Ring Down Spectroscopy with 5×10-13 cm-1 sensitivity. J Chem Phys 2012;137:234201. https://doi.org/10.1063/1.4769974.

26. Konefał M, Mondelain D, Kassi S, Campargue A. High sensitivity spectroscopy of the O2 band at 1.27 μm: (I) pure O2 line parameters above 7920 cm−1. J Quant Spectrosc Radiat Transfer 2020;241:106653. https://doi.org/10.1016/j.jqsrt.2019.106653.
27. Mondelain D, Mikhailenko SN, Karlovets EV, Béguier S, Kassi S, Campargue A. Comb-Assisted Cavity Ring Down Spectroscopy of 17O enriched water between 7443 and 7921 cm-1. J Quant Spectrosc Radiat Transfer 2017;203:206–12. https://doi.org/10.1016/j.jqsrt.2017.03.029.
28. Kassi S, Stoltmann T, Casado M, Daëron M, Campargue A. Lamb dip CRDS of highly saturated transitions of water near 1.4 μm. J Chem Phys 2018;148:054201. https://doi.org/10.1063/1.5010957.
29. Di Lonardo G, Fusina L, Tamassia F, Fayt A, Robert S, Vander Auwera J and Herman M. The FT absorption spectrum of $^{13}CH^{12}CH$ (III): vibrational states in the range 6750 to 9500 cm^{-1}. Mol Phys 2008;106:1161–1169.
30. Liévin J, Abbouti Temsamani M, Gaspard P, Herman M, Overtone spectroscopy and dynamics in monodeuteroacetylene (C_2HD). Chemical Physics 1995;190:419-445.
31. Cané E, Fusina L, Tamassia F, Fayt A, Herman M, Robert S, Vander Auwera J. The FT absorption spectrum of $^{13}CH^{12}CH$: rotational analysis of the vibrational states from 3800 to 6750 cm^{-1}. Mol Phys 2006;104:515–26.
32. Perevalov VI, Lukashevskaya AA. Parameterization of the effective dipole moment matrix elements in the case of the asymmetric top molecules. Application to NO2 molecule. Atmos Ocean Opt 2015;28:17–23.

Table 1.
Spectroscopic parameters (in cm^{-1}) of the rovibrational bands of acetylene assigned in the CRDS spectra of acetylene between 8203 and 8680 cm^{-1}. The bands are listed according to the increasing values of the upper state energy levels.

$v_1v_2v_3v_4v_5l_4l_5\varepsilon$ [a]	G_c	$B_{e/f}$	$D_{e/f}\times10^6$	$H_{e/f}\times10^{10}$	n_{fit}/N_{tot} [b]	Bands [c]	*Band type*	ΔG_c [d]	*Obsbserved lines* [e]	*rms* [f]	Previous reports [g]
$^{12}C_2H_2$											
0000000	0.0	1.1766462	1.6270	0.016							
0001010f	611.693755	1.18055377	1.67973	0.0187							
0001010e	611.693759	1.17532307	1.6405	0.0177							
0000101e	729.15410	1.1764413	1.6326	0.017							
0000101f	729.15410	1.1811398	1.6714	0.018							
0002020f	1228.7997	1.179109	1.692								
0002020e	1228.8011	1.17908	19.0	245							
0002000	1230.3894	1.17937	-15.8	-246							
000111-1e	1328.0722	1.180508	3.595	2.76							
000111-1f	1340.5507	1.1800836	1.715								
0001111f	1342.8023	1.179838	1.647								
0001111e	1342.8034	1.179804	-0.226	-2.78							
0000200	1449.1107	1.181234	4.415	6.52							
0000202f	1458.2936	1.180757	1.669								
0000202e	1458.2944	1.180714	-1.052	-6.43							
0003030e	1851.3699	1.180358	10.15								
0003030f	1851.3749	1.18006	6.33	39							
0003010f	1854.5970	1.18583	-3.8	-61							
0003010e	1854.5978	1.17533	-6.2								
***P*=13**											
N 020612-1f	8241.892(2)	1.18303(2)	-4.51(7)		11/13	$2\nu_2+(6\nu_4+\nu_5)^1II$	$\Pi_u-\Sigma_g^+$	8241.892(1)	Q17	1.6	
N 020612-1e	8241.9288(9)	1.16286(3)	-18.1(3)		21/24	$2\nu_2+(6\nu_4+\nu_5)^1II$	$\Pi_u-\Sigma_g^+$	8241.9288(9)	P13/R11	1.6	
N 011501 0f	8281.972(2)	1.17855(4)	-3.8(2)	-80(4)	15/16	$\nu_2+\nu_3+5\nu_4^1$	$\Pi_u-\Sigma_g^+$	8281.972(2)	Q19	1.2	
N 011501 0e	8281.9805(6)	1.163805(5)	-8.759(9)		35/39	$\nu_2+\nu_3+5\nu_4^1$	$\Pi_u-\Sigma_g^+$	8281.9806(6)	P23/R24	2.5 **P**	
N 030311-1e	8320.745(1)	1.16410(2)	-4.16(9)		11/12	$3\nu_2+(3\nu_4+\nu_5)^{0+}$	$\Sigma_u^+-\Sigma_g^+$	8320.745(1)	P19/R11	1.9	
1013030e	8329.277(4)	1.1693(2)	58(3)	1387(130)	15/45	$\nu_1+\nu_3+3\nu_4^3$	$\Phi_u-\Sigma_g^+$	8329.277(4)	P35/R32	0.4 **P**	
1013030f	8329.303(2)	1.16728(5)	8.4(4)	100(8)	14/23	$\nu_1+\nu_3+3\nu_4^3$	$\Phi_u-\Sigma_g^+$	8329.303(2)	Q27	1.9 **P**	
1013010e	8330.065(1)	1.16283(7)	-50(1)	-1175(46)	23/54	$\nu_1+\nu_3+3\nu_4^1$	$\Pi_u-\Sigma_g^+$	8330.065(1)	P35/R27	1.0 **P**	Lyu16, DB17
0212000e	8376.9721(7)	1.16117(3)	-11.7(2)	-133(4)	33/33	$2\nu_2+\nu_3+2\nu_4^0$	$\Sigma_u^+-\Sigma_g^+$	8376.9721(7)	P19/R15	1.3	Lyu16, DB17
002212-1f	8396.244(1)	1.17189(4)	4.7(4)	107(8)	12/21	$2\nu_3+(2\nu_4+\nu_5)^1II$	$\Pi_u-\Sigma_g^+$	8396.244(1)	Q21	1.7 **P**	Lyu16, DB17
N 002212-1e	8396.2455(9)	1.17132(2)	2.99(7)		18/18	$2\nu_3+(2\nu_4+\nu_5)^1II$	$\Pi_u-\Sigma_g^+$	8396.2455(9)	P17/R11	1.4	

	0022101f	8398.6876(9)	1.17499(1)	2.58(2)		16/19	$2\nu_3+(2\nu_4+\nu_5)^1$I	$\Pi_u - \Sigma_g^+$	8398.6876(9)	Q22	1.8	Lyu16, DB17
	0022101e	8398.6982(7)	1.169929(5)	0.257(7)		30/44	$2\nu_3+(2\nu_4+\nu_5)^1$I	$\Pi_u - \Sigma_g^+$	8398.6982(7)	P28/R26	2.1 **P**	
N	110412-1e	8412.0180(7)	1.17046(1)	3.50(3)		27/27	$\nu_1+\nu_2+(4\nu_4+\nu_5)^1$II	$\Pi_u - \Sigma_g^+$	8412.0180(7)	P20/R17	1.7	
	110412-1f	8412.0254(9)	1.174805(9)	2.04(2)		19/19	$\nu_1+\nu_2+(4\nu_4+\nu_5)^1$II	$\Pi_u - \Sigma_g^+$	8412.0254(9)	Q23	1.3	Lyu16, DB17
N	1104101e	8439.197(2)	1.17429(5)	1.4(3)		7/7	$\nu_1+\nu_2+(4\nu_4+\nu_5)^1$I	$\Pi_u - \Sigma_g^+$	8439.197(2)	P14/R10	2.2	
N	1104101f	8439.222(1)	1.17098(1)	-0.32(3)		6/7	$\nu_1+\nu_2+(4\nu_4+\nu_5)^1$I	$\Pi_u - \Sigma_g^+$	8439.222(1)	Q23	1.4	
	1110000e	8512.0567(4)	1.157897(1)	1.6336(5)		90/93	$\nu_1+\nu_2+\nu_3$	$\Sigma_u^+ - \Sigma_g^+$	8512.0567(4)	P50/R44	0.8	HIT16, Lyu16, DB17
N	0400101e	8530.8579(5)	1.151306(3)	1.650(2)		30/31	$4\nu_2+\nu_5^1$	$\Pi_u - \Sigma_g^+$	8530.8579(5)	P16/R36	1.8	
N	1011210e	8531.5722(7)	1.165254(6)	2.51(1)		32/32	$\nu_1+\nu_3+(\nu_4+2\nu_5)^1$II	$\Pi_u - \Sigma_g^+$	8531.5722(7)	P19/R23	1.4	
	120111-1e	8556.5913(5)	1.161948(4)	4.413(6)	5.41(3)	66/74	$\nu_1+2\nu_2+(\nu_4+\nu_5)^{0+}$	$\Sigma_u^+ - \Sigma_g^+$	8556.5913(5)	P41/R39	1.3	HIT16, Lyu16, DB17
N	10112-12e	8556.927(2)	1.17194(4)	1.8(1)		7/8	$\nu_1+\nu_3+(\nu_4+2\nu_5)^1$I	$\Pi_u - \Sigma_g^+$	8556.927(2)	P15/R15	1.7	
N	10112-12f	8556.932(1)	1.16722(1)	1.57(3)		10/10	$\nu_1+\nu_3+(\nu_4+2\nu_5)^1$I	$\Pi_u - \Sigma_g^+$	8556.932(1)	Q22	1.6	
	1201111e	8569.446(1)	1.161388(7)	-0.65(1)	-4.72(6)	33/37	$\nu_1+2\nu_2+(\nu_4+\nu_5)^2$	$\Delta_u - \Sigma_g^+$	8569.446(1)	P39/R32	1.1	
	200212-1f	8580.2989(7)	1.172236(7)	3.16(2)		22/22	$2\nu_1+(2\nu_4+\nu_5)^1$II	$\Pi_u - \Sigma_g^+$	8580.2989(7)	Q23	1.2	
	200212-1e	8580.2998(7)	1.16544(1)	3.03(3)		27/30	$2\nu_1+(2\nu_4+\nu_5)^1$II	$\Pi_u - \Sigma_g^+$	8580.2998(7)	P17/R20	1.5	
	030131-1e	8581.7622(6)	1.164991(9)	7.11(3)		33/34	$3\nu_2+(\nu_4+3\nu_5)^{0+}$	$\Sigma_u^+ - \Sigma_g^+$	8581.7622(6)	P21/R17	1.4	Lyu16, DB17
	2002101f	8597.3033(9)	1.167436(5)	2.438(6)		20/29	$2\nu_1+(2\nu_4+\nu_5)^1$I	$\Pi_u - \Sigma_g^+$	8597.3033(9)	Q29	1.5	Lyu16, DB17
	2002101e	8597.3039(6)	1.169094(6)	2.10(2)		37/38	$2\nu_1+(2\nu_4+\nu_5)^1$I	$\Pi_u - \Sigma_g^+$	8597.3039(6)	P21/R21	0.9	Lyu16, DB17
	021020 0e	8640.1399(6)	1.162897(8)	3.82(2)		35/36	$2\nu_2+\nu_3+2\nu_5^0$	$\Sigma_u^+ - \Pi_u$	8640.1399(6)	P23/R13	1.3	Lyu16, DB17
	***P*=14**											
N	011602 0f	8901.605(1)	1.17347(3)			6/7	$\nu_2+\nu_3+6\nu_4^2-\nu_4^1$	$\Delta_u - \Pi_g$	8289.9169(9)	P10/R5	1.0	
N	011602 0e	8901.707(2)	1.16897(4)	18.0(2)		12/15	$\nu_2+\nu_3+6\nu_4^2-\nu_4^1$	$\Delta_u - \Pi_g$	8290.0109(9)	P10/Q13/R13	2.2	
N	021301 0f	8969.6947(8)	1.16814(1)	-0.92(4)		22/28	$2\nu_2+\nu_3+3\nu_4^1-\nu_4^1$	$\Pi_u - \Pi_g$	8358.0009(9)	P20/Q10/R11	2.0	
N	021301 0e	8969.7012(6)	1.156818(8)	-4.96(2)		24/28	$2\nu_2+\nu_3+3\nu_4^1-\nu_4^1$	$\Pi_u - \Pi_g$	8358.0074(7)	P24/Q18/R13	2.0	
N	020535-3f	8973.838(1)	1.17476(1)	4.41(2)		9/12	$2\nu_2+(5\nu_4+3\nu_5)^2$IV$-\nu_4^1$	$\Delta_u - \Pi_g$	8362.143(1)	P15/R25	2.0	
N	020535-3e	8973.855(1)	1.17433(6)	17.7(3)		6/6	$2\nu_2+(5\nu_4+3\nu_5)^2$IV$-\nu_4^1$	$\Delta_u - \Pi_g$	8362.160(1)	P5/R13	1.6	
N	002311-1f	8996.898(1)	1.17278(4)	8.7(3)		9/10	$2\nu_3+(3\nu_4+\nu_5)^0-\nu_4^1$	$\Sigma_u^- - \Pi_g$	8385.205(1)	P13/R11	1.4	
N	0121010f	9046.898(1)	1.16393(2)	1.66(6)		7/10	$\nu_2+2\nu_3+\nu_4^1-\nu_5^1$	$\Pi_g - \Pi_u$	8317.747(1)	P19/R17	0.8	
N	0121010e	9046.906(1)	1.15738(1)	1.66(2)		12/12	$\nu_2+2\nu_3+\nu_4^1-\nu_5^1$	$\Pi_g - \Pi_u$	8317.7543(9)	P24/Q8/R8	1.7	
	1111010e	9084.9955(4)	1.156660(1)	1.6498(9)		88/96	$\nu_1+\nu_2+\nu_3+\nu_4^1-\nu_4^1$	$\Pi_u - \Pi_g$	8473.3018(4)	P43/Q38/R37	1.4	Lyu16, DB17
	1111010f	9084.9965(4)	1.162328(3)	1.741(2)		48/74	$\nu_1+\nu_2+\nu_3+\nu_4^1-\nu_4^1$	$\Pi_u - \Pi_g$	8473.3021(4)	P40/Q32/R32	1.2 **P**	Lyu16, DB17
N	0212101f	9094.830(2)	1.16241(1)	3.63(1)		5/8	$2\nu_2+\nu_3+(2\nu_4+\nu_5)^1I-\nu_5^1$	$\Pi_g - \Pi_u$	8365.677(2)	P30/R4	1.0	
N	0212101e	9094.837(1)	1.162578(2)			8/10	$2\nu_2+\nu_3+(2\nu_4+\nu_5)^1I-\nu_5^1$	$\Pi_g - \Pi_u$	8365.684(1)	P29/R18	1.8	
	030232-1f [h]	9127.3120(7)	1.170115(6)	4.104(8)		34/42	$3\nu_2+(2\nu_4+3\nu_5)^1$III$-\nu_4^1$	$\Pi_u - \Pi_g$	8515.6194(6)	P37/Q11/R30	1.7	DB17
	030232-1e [h]	9127.3160(6)	1.158724(6)	2.78(1)		40/44	$3\nu_2+(2\nu_4+3\nu_5)^1$III$-\nu_4^1$	$\Pi_u - \Pi_g$	8515.6226(5)	P24/Q11/R20	1.2	DB17
N	120212-1e	9142.9970(9)	1.163485(6)	4.130(8)		22/27	$\nu_1+2\nu_2+(2\nu_4+\nu_5)^1II-\nu_4^1$	$\Pi_u - \Pi_g$	8531.303(1)	P30/R25	1.8	

N	1202101f	9152.797(1)	1.16681(1)	1.27(3)		17/23	$\nu_1+2\nu_2+(2\nu_4+\nu_5)^1\mathrm{I}-\nu_4^1$	$\Pi_u-\Pi_g$	8541.104(1)	P16/R22	2.2	**P**	
N	1202101e	9152.822(1)	1.16117(3)	1.6(1)		13/15	$\nu_1+2\nu_2+(2\nu_4+\nu_5)^1\mathrm{I}-\nu_4^1$	$\Pi_u-\Pi_g$	8541.129(1)	P14/R14	2.2	**P**	
	0120101e	9177.3602(6)	1.15885(1)	1.85(4)	5.0(4)	44/45	$\nu_2+2\nu_3+\nu_5^1-\nu_4^1$	$\Pi_u-\Pi_g$	8565.6658(6)	P24/Q10/R25	1.4		
	0120101f	9177.3619(5)	1.163911(4)	1.650(6)		45/46	$\nu_2+2\nu_3+\nu_5^1-\nu_4^1$	$\Pi_u-\Pi_g$	8565.6685(4)	P27/Q11/R27	1.5		
	0211210f	9213.109(1)	1.16854(2)	2.55(4)		14/14	$2\nu_2+\nu_3+(\nu_4+2\nu_5)^1\mathrm{II}-\nu_4^1$	$\Pi_u-\Pi_g$	8601.416(1)	P17/R18	1.3		
	0211210e	9213.111(3)	1.15886(5)	2.1(2)		7/8	$2\nu_2+\nu_3+(\nu_4+2\nu_5)^1\mathrm{II}-\nu_4^1$	$\Pi_u-\Pi_g$	8601.419(1)	P16/R16	2.0		
	1110101f	9215.7170(4)	1.162648(2)	1.7426(9)		60/67	$\nu_1+\nu_2+\nu_3+\nu_5^1-\nu_5^1$	$\Pi_g-\Pi_u$	8486.5629(4)	P41/R32	1.5		Lyu16, DB17
	1110101e	9215.7283(6)	1.157663(8)	2.17(2)	3.1(2)	52/64	$\nu_1+\nu_2+\nu_3+\nu_5^1-\nu_5^1$	$\Pi_g-\Pi_u$	8486.5721(6)	P31/Q13/R30	2.3		Lyu16, DB17
	2101010e	9238.4560(5)	1.156152(3)	1.627(3)		56/60	$2\nu_1+\nu_2+\nu_4^1-\nu_5^1$	$\Pi_g-\Pi_u$	8509.3024(5)	P34/Q7/R30	1.7		Lyu16, DB17
	2101010f	9238.4575(4)	1.161200(2)	1.637(2)		59/67	$2\nu_1+\nu_2+\nu_4^1-\nu_5^1$	$\Pi_g-\Pi_u$	8509.3033(4)	P35/Q15/R35	1.3		Lyu16, DB17
N	1201210f	9260.8305(6)	1.169798(3)	3.250(2)		29/45	$\nu_1+2\nu_2+(\nu_4+2\nu_5)^1\mathrm{II}-\nu_5^1$	$\Pi_g-\Pi_u$	8531.6761(6)	P33/R33	1.9	**P**	
N	1201210e	9260.8320(5)	1.158906(3)	2.497(3)		41/45	$\nu_1+2\nu_2+(\nu_4+2\nu_5)^1\mathrm{II}-\nu_5^1$	$\Pi_g-\Pi_u$	8531.6780(5)	P29/R32	2.6		
N	12012-12e	9280.836(1)	1.16541(2)	1.85(5)		12/16	$\nu_1+2\nu_2+(\nu_4+2\nu_5)^1\mathrm{I}-\nu_5^1$	$\Pi_g-\Pi_u$	8551.681(1)	P17/R20	1.6		
N	12012-12f	9280.847(3)	1.16062(4)	1.5(1)		7/10	$\nu_1+2\nu_2+(\nu_4+2\nu_5)^1\mathrm{I}-\nu_5^1$	$\Pi_g-\Pi_u$	8551.692(3)	P14/R14	1.2		
	***P*=15**												
	0030000e	9639.8693(8)	1.15837(2)	1.86(5)		20/22	$3\nu_3-2\nu_4^0$	$\Sigma_u^+-\Sigma_g^+$	8409.4799(8)	P15/R16	2.2		
	1112020e	9664.333(1)	1.16089(3)	8.6(1)		27/51	$\nu_1+\nu_2+\nu_3+2\nu_4^2-2\nu_4^2$	$\Delta_u-\Delta_g$	8435.531(1)	P29/Q18/R33	1.8	**P**	
	1112020f	9664.3330(5)	1.160929(3)	1.726(3)		40/51	$\nu_1+\nu_2+\nu_3+2\nu_4^2-2\nu_4^2$	$\Delta_u-\Delta_g$	8435.5329(5)	P34/Q13/R30	1.4		
	1112000e	9668.1617(8)	1.16126(2)	-4.84(9)		20/54	$\nu_1+\nu_2+\nu_3+2\nu_4^0-2\nu_4^0$	$\Sigma_u^+-\Sigma_g^+$	8437.772(8)	P37/R39	2.0	**P**	
N	111111-1e	9774.999(1)	1.16229(1)	4.09(2)		13/14	$\nu_1+\nu_2+\nu_3+(\nu_4+\nu_5)^0-(\nu_4+\nu_5)^0$	$\Sigma_u^+-\Sigma_g^+$	8446.927(1)	P24	1.9		
N	111111 1e	9787.7556(7)	1.161582(5)	-0.377(7)		38/44	$\nu_1+\nu_2+\nu_3+(\nu_4+\nu_5)^2-(\nu_4+\nu_5)^2$	$\Delta_g-\Delta_u$	8444.9526(7)	P27/Q26/R21	2.0		
N	1111111f	9787.7590(6)	1.161494(6)	1.88(1)		39/42	$\nu_1+\nu_2+\nu_3+(\nu_4+\nu_5)^2-(\nu_4+\nu_5)^2$	$\Delta_g-\Delta_u$	8444.9574(6)	P25/Q24/R20	1.9		
N	111111-1f	9794.3406(6)	1.161593(3)	1.721(2)		39/43	$\nu_1+\nu_2+\nu_3+(\nu_4+\nu_5)^0-(\nu_4+\nu_5)^0$	$\Sigma_u^--\Sigma_g^-$	8453.7900(6)	P36/R21	1.5		
N	1110200e	9909.9098(7)	1.162473(8)	4.32(2)		24/33	$\nu_1+\nu_2+\nu_3+2\nu_5^0-2\nu_5^0$	$\Sigma_u^+-\Sigma_g^+$	8460.798(1)	P25/R27	1.9	**P**	
N	1110202e	9920.3451(7)	1.162021(6)	-0.619(7)		20/25	$\nu_1+\nu_2+\nu_3+2\nu_5^2-2\nu_5^2$	$\Delta_u-\Delta_g$	8462.0505(7)	P30/Q12/R19	2.1		
N	1110202f	9920.362(2)	1.16182(1)	1.48(1)		13/20	$\nu_1+\nu_2+\nu_3+2\nu_5^2-2\nu_5^2$	$\Delta_u-\Delta_g$	8462.067(2)	P30/R17	1.5		
	***P*=16**												
N	1113010e	10255.382(2)	1.1575(1)	-4(1)		6/8	$\nu_1+\nu_2+\nu_3+3\nu_4^1-3\nu_4^1$	$\Pi_u-\Pi_g$	8400.784(2)	P12	2.4		
N	1113010f	10255.390(1)	1.16877(2)	-3.2(1)	-63(1)	14/16	$\nu_1+\nu_2+\nu_3+3\nu_4^1-3\nu_4^1$	$\Pi_u-\Pi_g$	8400.793(1)	P24/R11	2.0		
$^{13}C^{12}CH_2$													
	0000000	0.0	1.1484335	1.5256									
	0001010e	608.3535	1.147100	1.592									
	0001010f	608.3535	1.152127	1.640									
	***P*=13**												
	021111-1e	8414.8195(6)	1.132925(4)	2.149(4)		36/44	$\nu_2+\nu_3+\nu_4^1$	$\Sigma-\Sigma$	8414.8195(6)	P32/R26	1.1		Dilo08
	0120000e	8435.2178(5)	1.132399(5)	6.04(1)	30.82(7)	49/49	$\nu_2+2\nu_3$	$\Sigma-\Sigma$	8435.2178(5)	P33/R34	1.8		Dilo08

1110000e	8464.2280(5)	1.132370(2)	2.700(5)	3.05(2)	60/64	$\nu_1+\nu_2+\nu_3$	Σ – Σ	8464.2280(5)	P45/R33	1.7	Dilo08, Lyu16, DB17
030131-1e	8475.6845(5)	1.134848(3)	5.706(5)	12.66(2)	54/55	$3\nu_2+(\nu_4+3\nu_5)^{0+}$	Σ – Σ	8475.6845(5)	P36/R28	1.7	Dilo08, Lyu16, DB17
120111-1e	8491.4420(6)	1.134271(6)	4.73(2)	9.4(1)	37/40	$\nu_1+2\nu_2+(\nu_4+\nu_5)^{0+}$	Σ – Σ	8491.4420(6)	P32/R21	1.4	Dilo08, Lyu16, DB17
2100000e	8607.801(1)	1.13030(2)	1.74(5)		15/17	$2\nu_1+\nu_2$	Σ – Σ	8607.801(1)	P14/R17	1.8	Dilo08
***P*=14**											
1111010f	9030.7878(7)	1.141389(4)	4.998(3)		28/36	$\nu_1+\nu_2+\nu_3+\nu_4^1-\nu_4^1$	Π – Π	8419.0939(8)	P28/R33	1.9	Dilo08
1111010e	9030.7903(7)	1.130830(9)	2.48(2)		29/35	$\nu_1+\nu_2+\nu_3+\nu_4^1-\nu_4^1$	Π – Π	8419.0960(9)	P22/R18	1.9	Dilo08
C_2HD											
0000000	0.0	0.991538	1.141								
2100000e	8409.3045(9)	0.977648(9)	1.12(2)		24/28	$2\nu_1+\nu_2$	Σ – Σ	8409.3045(9)	P24/R20	1.8	Liev95

Notes

The confidence interval (1 SD) is given in parenthesis in the unit of the last quoted digit. The parameters of the lower vibrational levels of $^{12}C_2H_2$, $^{12}C^{13}CH_2$ and $^{12}C_2HD$ (grey background) were constrained to their fitted values of Ref. [13], Ref. [31] and Ref. [30], respectively.

[a] Normal mode labeling: $v_{i=1-5}$ are the vibrational quantum numbers, $l_{4,5}$ are the vibrational angular momentum quantum numbers associated to the degenerate bending modes and $\varepsilon=e$ or f is the symmetry type relative to the Wang transformation. The labeling was obtained according to the maximum value of the modulo of the expansion coefficients of the vibrational eigenfunction in the normal mode basis (for low J values). In a few cases of the same main contributors different labeling has been chosen (see Text, Section 3). "N" marks upper states newly observed.

[b] N_{tot} is the total number of the observed transitions reaching a given vibrational state and n_{fit} is the number of positions included in the fit of the parameters.

[c] Observed band in Plíva notation. (see Text, Section 3).

[d] Band center. $\Delta G_c = G_c^{'} - G_c^{''}$

[e] Observed branches with the maximum value of the total angular momentum quantum number.

[f] Root mean square deviation in 10^{-3} cm^{-1} unit. "P" marks perturbed states

[g] Reference to previous reports: HIT16 [1], Lyu16 [10], DB17 [15], Dilo08 [29], Liev95 [30].

[h] The labeling differs from that of the reference DB17 [15] (see Text, Section 3).

Table 2
The obtained values of the vibrational transition dipole moment squared and Herman-Wallis factors. Only band center and approximate value of the vibrational transition dipole moment squared are given for the bands where the fit of intensities failed. The bands are ordered according to their band centers.

ISO [a]	Band [b]	ΔG_c [c]	N_{exp} [d]	*rms (%)* [e]	N_{tot} [f]	Transitions [g]	$\|R_0\|^2$ *in* D^2	$A_1^{PR}\times10^2$	$A_2^{PR}\times10^3$	$A_2^{Q}\times10^3$	Note [h]	Unc.% [i]
261	020612-1 - 0000000	8241.91	19	6.0	40	P13/Q17/R11	$2.90(4)\times10^{-11}$					7
261	0115010 - 0000000	8281.97	34	9.3	61	P23/Q24/R19	$1.32(2)\times10^{-10}$	-0.82(8)				10
261	0116020 - 0001010	8290.00			21		$1.0(2)\times10^{-10}$					20
261	0121010 - 0000101	8317.75			22		$4.3(8)\times10^{-10}$					20
261	030311-1 - 0000000	8320.75			12		$8(2)\times10^{-12}$					20
261	1013030 - 0000000	8329.29	19	12	71	P35/Q27/R32	$1.8(2)\times10^{-11}$	-14(2)	58(5)	24(3)		15
261	1013010 - 0000000	8330.00	22	6.2	55	P35/R27	$2.20(5)\times10^{-9}$	-0.85(7)	-1.73(9)			10
261	0213010 - 0001010	8358.01			56		$1.30(6)\times10^{-9}$		-0.76(9)			20
261	020535-3 - 0001010	8362.15			18		$4.2(9)\times10^{-10}$					20
261	0211210 - 0001010	8365.67			22		$8.4(7)\times10^{-10}$					20
261	0212101 - 0000101	8365.68			18		$6(1)\times10^{-10}$					20
261	0212000 - 0000000	8376.97	25	4.1	37	P20/R16	$4.34(6)\times10^{-10}$		-0.34(4)			5
261	002311-1f - 0001010	8385.21			11		$9(2)\times10^{-10}$					20
261	002212-1 - 0000000	8396.24	26	5.6	50	P17/Q21/R12	$4.09(7)\times10^{-10}$		-1.65(6)	0.90(6)		7
261	0022101 - 0000000	8398.69	41	6.2	72	P28/Q22/R27	$7.0(1)\times10^{-10}$		0.68(4)	-1.28(4)		7
261	1113010 - 0003010	8400.79			24		$2.4(2)\times10^{-7}$					20
263	2100000 - 0000000	8409.30			28		$1.11(8)\times10^{-6}$					20
261	0030000 - 0002000	8409.48	12	7.2	33	P16/R16	$2.72(6)\times10^{-10}$					8
261	110412-1 - 0000000	8412.02	30	7.1	61	P20/Q24/R18	$6.7(1)\times10^{-10}$		-0.53(4)			10
262	021111-1 - 0000000	8414.82	28	7.5	54	P28/R26	$7.2(1)\times10^{-8}$					10
262	1111010 - 0001010	8419.09	30	10	91	P29/R33	$8.3(2)\times10^{-7}$					15
262	0120000 - 0000000	8435.22	31	8.1	56	P33/R34	$1.95(3)\times10^{-7}$					10
261	1112020 - 0002020	8435.53	54	5.9	113	P34/Q18/R33	$3.67(3)\times10^{-7}$					8
261	1112000 - 0002000	8437.77	29	9.7	60	P37/R39	$3.15(6)\times10^{-7}$					10
261	1104101 - 0000000	8439.20			14		$1.0(2)\times10^{-10}$					20
261	1111111 - 0001111	8444.95	40	10	118	P28/Q26/R22	$3.39(6)\times10^{-7}$					15
261	111111-1 - 000111-1	8450.00	31	11	72	P36/R22	$4.13(8)\times10^{-7}$					15
261	1110200 - 0000200	8460.80	20	7.5	50	P25/R27	$2.96(5)\times10^{-7}$					10
261	1110202 - 0000202	8462.06	24	12	85	P30/Q12/R19	$3.51(9)\times10^{-7}$					15
262	1110000 - 0000000	8464.23	46	5.2	73	P45/R33	$1.80(2)\times10^{-6}$		0.18(1)		Lyu16	7
261	1111010 - 0001010	8473.30	90	5.0	180	P43Q38/R37	$4.37(2)\times10^{-7}$				Lyu16	10
262	030131-1 - 0000000	8475.68	45	5.0	64	P36/R29	$1.19(1)\times10^{-6}$		-0.06(1)		Lyu16	7
261	1110101 - 0000101	8486.57	88	5.3	143	P41/Q13/R32	$3.49(3)\times10^{-7}$		0.08(1)		Lyu16	5
262	120111-1 - 0000000	8491.44	26	8.0	49	P32/R21	$3.9(1)\times10^{-7}$		-0.19(5)		Lyu16	10
261	2101010 - 0000101	8509.30	85	7.4	148	P35/Q15/R35	$9.6(1)\times10^{-8}$		0.14(2)		Lyu16	7
261	1110000 - 0000000	8512.06	79	3.5	94	P50/R44	$5.32(2)\times10^{-7}$				HITRAN	5

261	030232-1 - 0001010	8515.62	57	4.4	124	P37/Q12/R30	$3.58(2)\times10^{-8}$					5
261	0400101 - 0000000	8530.86	16	6.8	48	P16/R36	$4.08(8)\times10^{-10}$	3.91(8)				10
261	120212-1 - 0001010	8531.30	13	9.0	38	P30/R25	$4.3(1)\times10^{-9}$					10
261	1011210 - 0000000	8531.57	22	6.2	44	P20/R24	$5.17(7)\times10^{-10}$	0.36(5)				7
261	1201210 - 0000101	8531.67	58	9.4	111	P33/R33	$3.54(4)\times10^{-8}$					15
261	1202101 - 0001010	8541.11	27	10	61	P16/R22	$5.4(1)\times10^{-9}$					15
261	12012-12 - 0000101	8551.69			26		$2.6(2)\times10^{-9}$					20
261	120111-1 - 0000000	8556.59	55	4.9	77	P41/R39	$2.64(2)\times10^{-8}$				HITRAN	7
261	10112-12 - 0000000	8556.93			18		$7(1)\times10^{-11}$					20
261	0120101 - 0001010	8565.67	68	7.4	128	P28/Q12/R28	$1.34(1)\times10^{-8}$			12.5(4)		8
261	1201111 - 0000000	8569.45	20	6.8	63	P39/R33	$2.4(3)\times10^{-11}$		14(1)			10
261	200212-1 - 0000000	8580.30	29	8.2	60	P17/Q24/R20	$5.9(1)\times10^{-10}$			-0.63(4)		10
261	030131-1 - 0000000	8581.76	25	6.1	38	P21/R17	$1.45(2)\times10^{-9}$	-0.43(6)			Lyu16	5
261	2002101 - 0000000	8597.30	48	6.8	71	P22/Q29/R21	$2.64(3)\times10^{-9}$				Lyu16	7
262	2100000 - 0000000	8607.80			17		$1.9(1)\times10^{-8}$					20
261	0210200 - 0000000	8640.14	21	5.1	39	P24/R14	$4.91(8)\times10^{-10}$		0.22(5)			5

Notes

[a] Isotopologue number following HITRAN notation: 261 ($^{12}C_2H_2$), 262 ($^{12}C^{13}CH_2$) and 263 ($^{12}C_2HD$)

[b] Band vibrational labeling, ($v_1v_2v_3v_4v_5\ell_4\ell_5$)

[c] Band center in cm^{-1}

[d] N_{exp} is the number of measured line intensities included in the fit of the Herman-Wallis coefficients. No value is given when the fit failed.

[e] Root mean square deviation of the intensity fit in %

[f] N_{tot} is the total number of lines included in our recommended list (SupMat 3)

[g] Maximum *J* value included in the database for the *P*, *Q* and *R* branches of each band

[h] The band was completed using indicated source: HITRAN2016 [1] or Lyu16 [10]

[i] Estimated uncertainties of the line intensities given in the recommended line list (SupMat 3).

Fig. 1

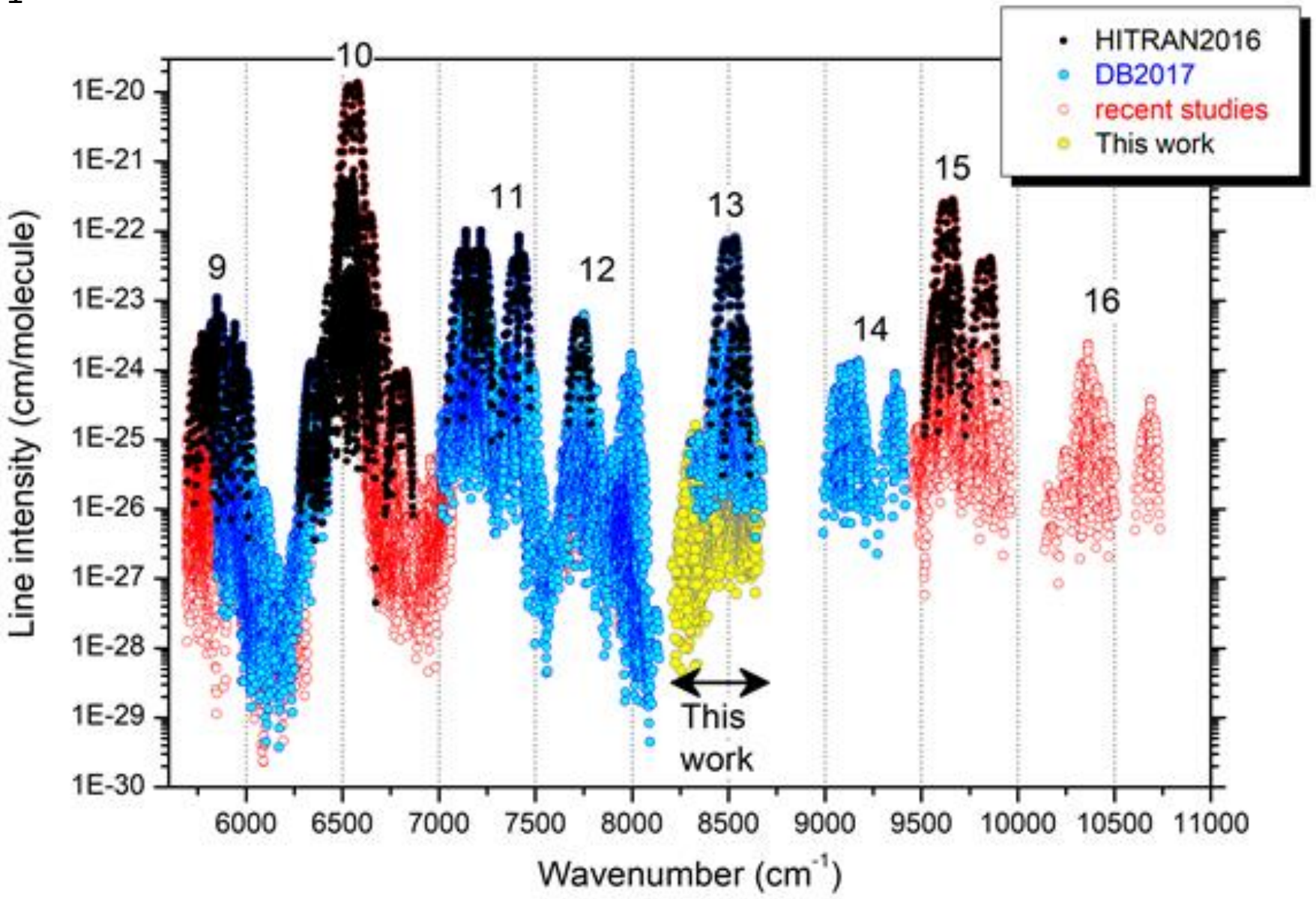

Fig. 2

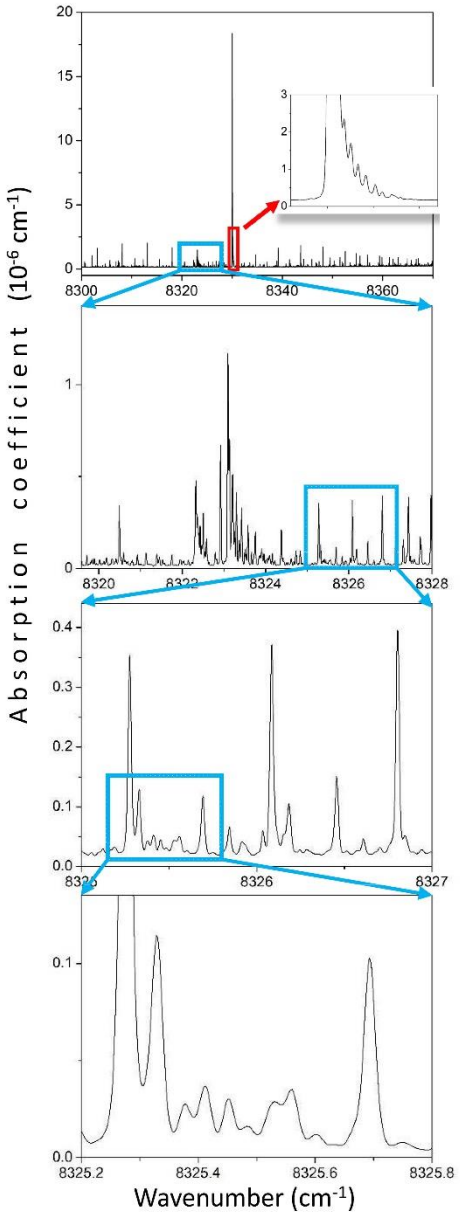
Absorption coefficient (10^{-6} cm^{-1})
Wavenumber (cm^{-1})
20
15
10
5
0
3
2
1
0
8300
8320
8340
8360
1
0
8320
8322
8324
8326
8328
0.4
0.3
0.2
0.1
0.0
8326
8327
0.1
0.0
8325.2
8325.4
8325.6
8325.8

Fig. 3

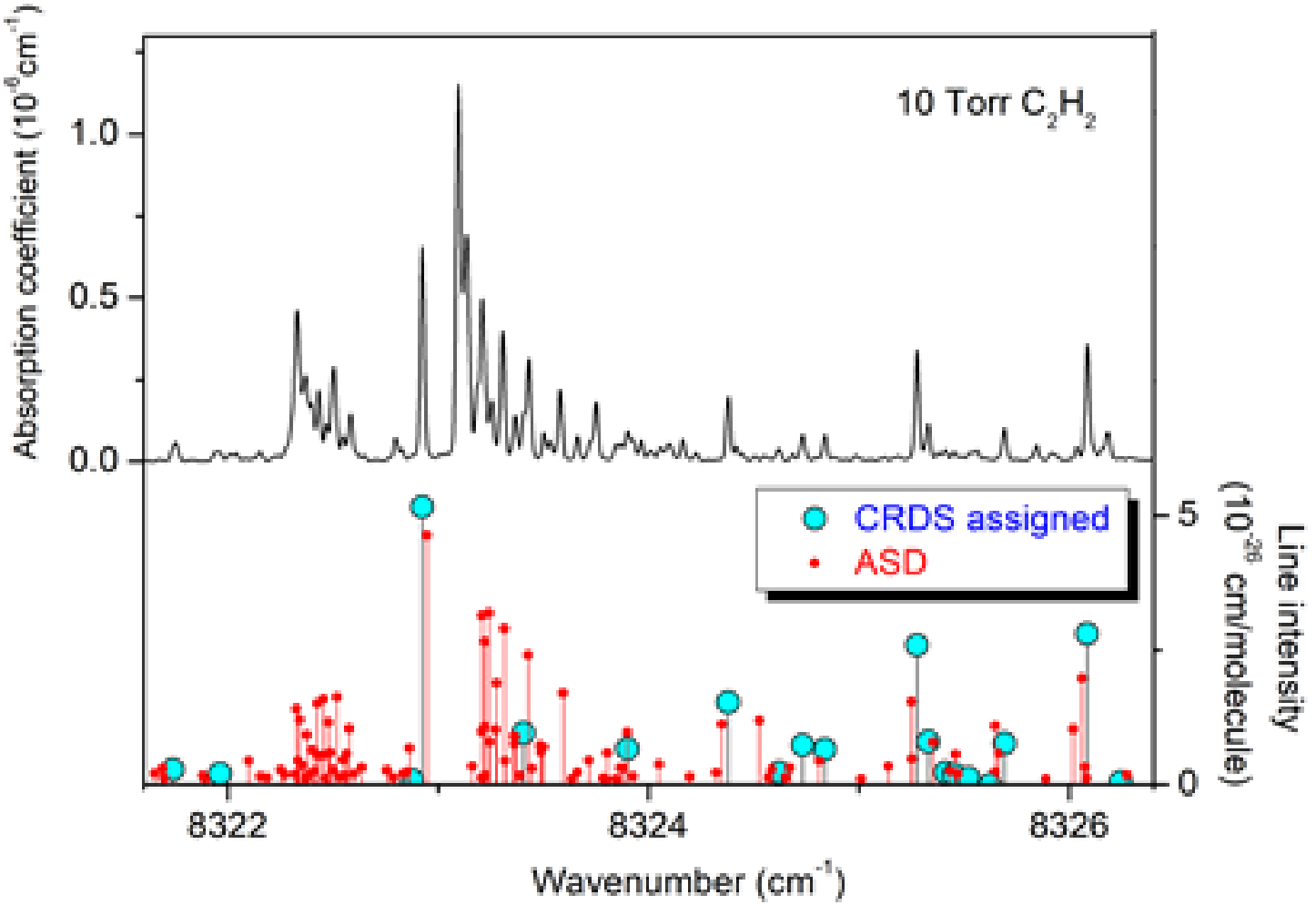
10 Torr C_2H_2
CRDS assigned
ASD
Absorption coefficient (10^{-6} cm^{-1})
Line intensity (10^{-26} cm/molecule)
Wavenumber (cm^{-1})
1.0
0.5
0.0
5
0
8322
8324
8326

Fig. 4

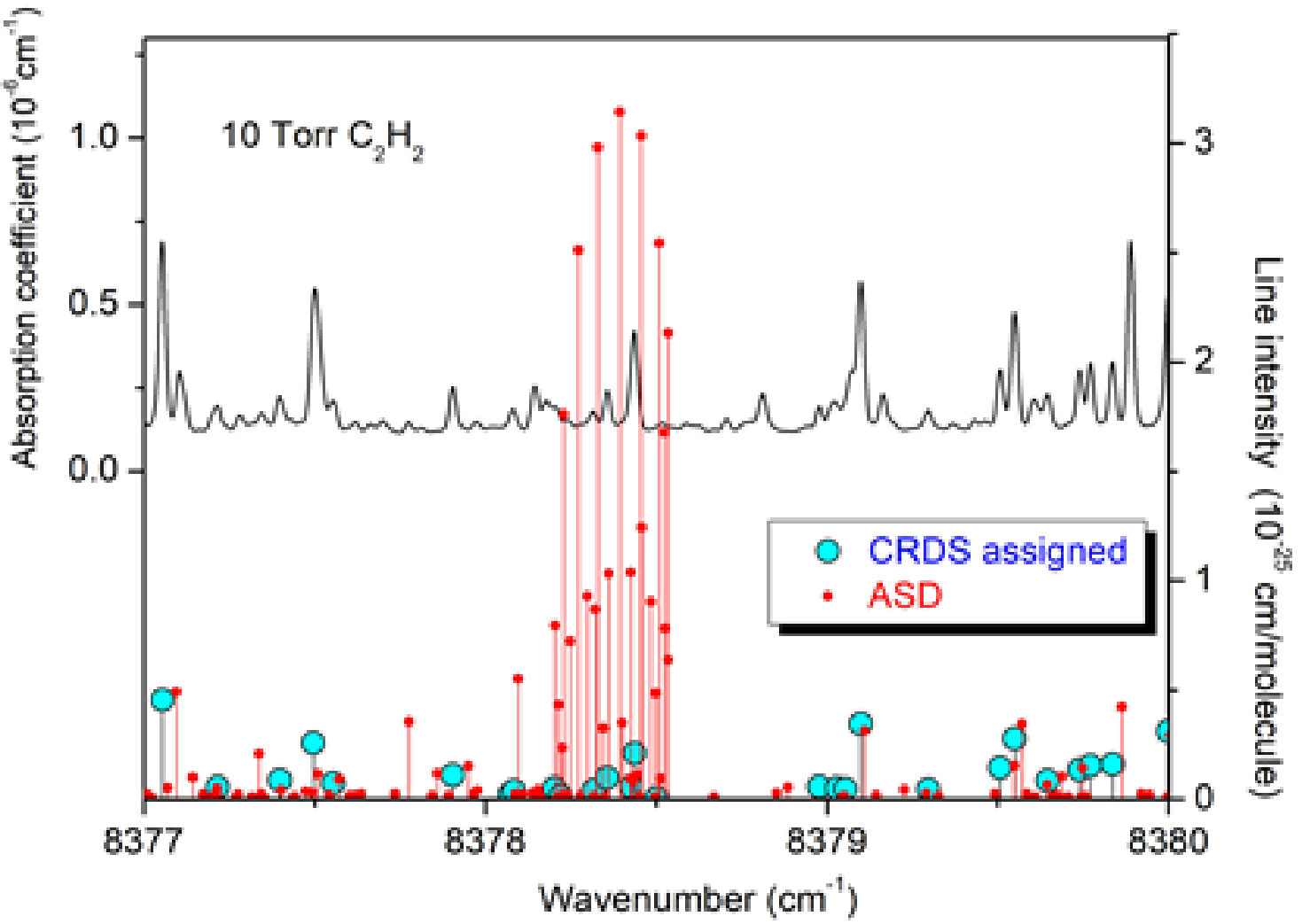
10 Torr C2H2
Absorption coefficient (10-6 cm-1)
Line intensity (10-25 cm/molecule)
Wavenumber (cm-1)
CRDS assigned
ASD
1.0
0.5
0.0
3
2
1
0
8377
8378
8379
8380

Fig. 5

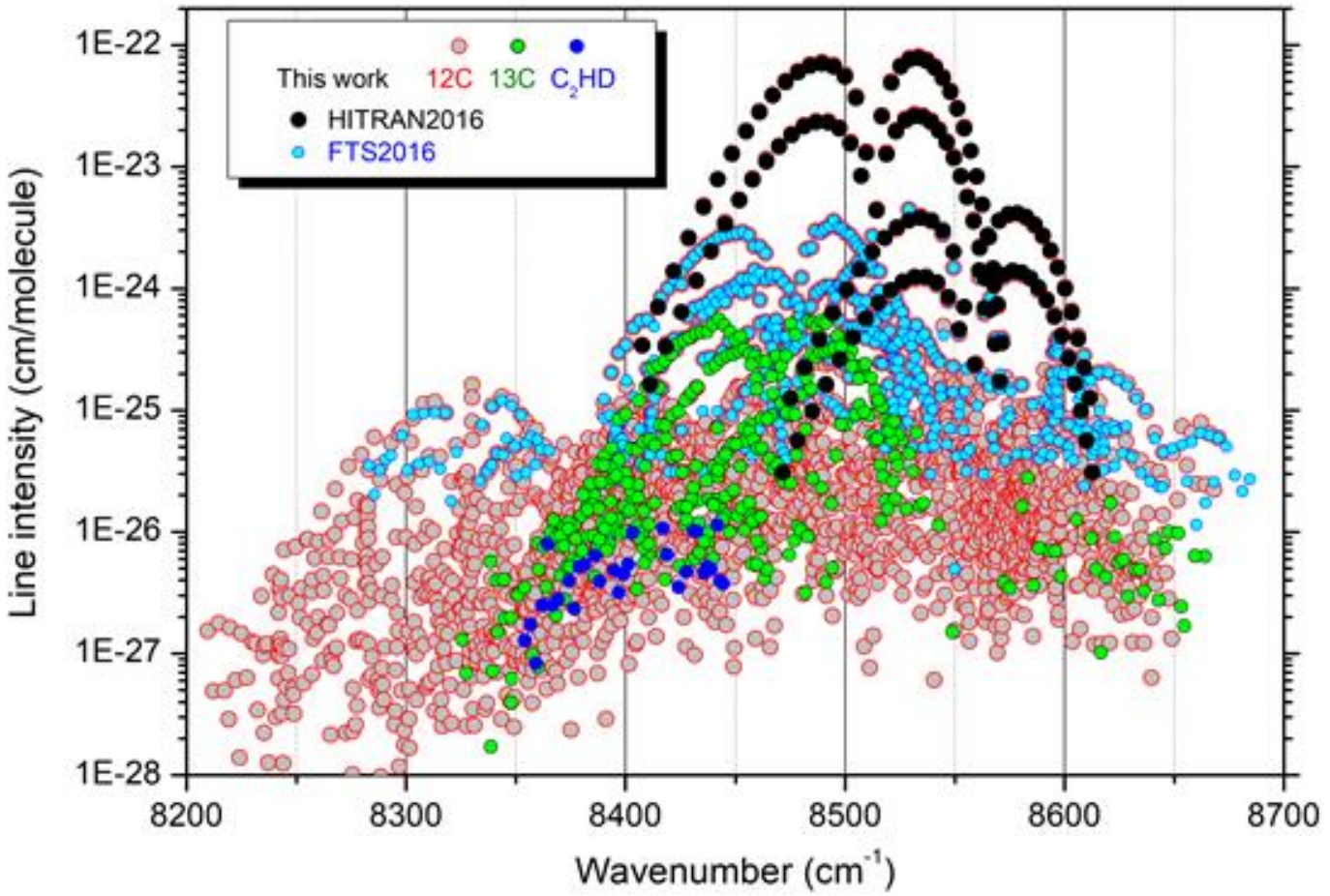
This work 12C 13C C2HD
HITRAN2016
FTS2016
Line intensity (cm/molecule)
1E-22
1E-23
1E-24
1E-25
1E-26
1E-27
1E-28
8200
8300
8400
8500
8600
8700
Wavenumber (cm-1)

Fig. 6

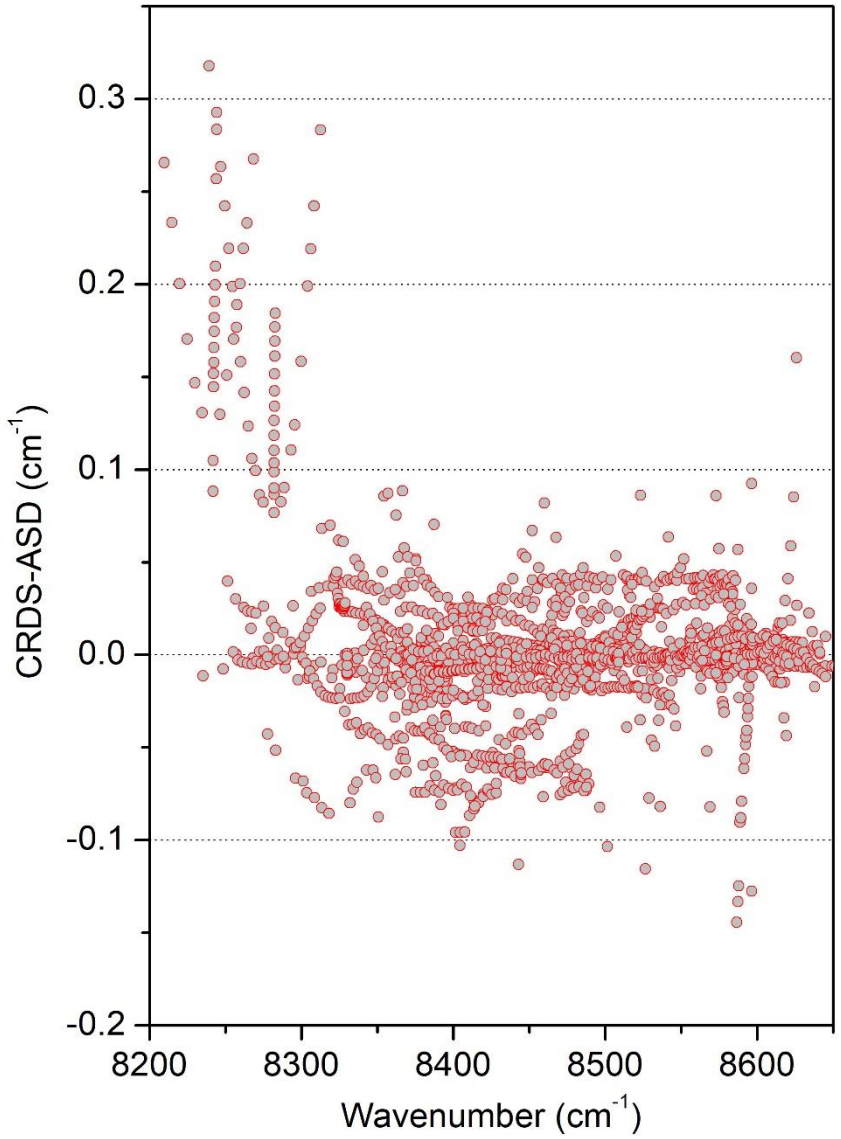
0.3
0.2
0.1
0.0
-0.1
-0.2
CRDS-ASD (cm-1)
8200
8300
8400
8500
8600
Wavenumber (cm-1)

Fig. 7

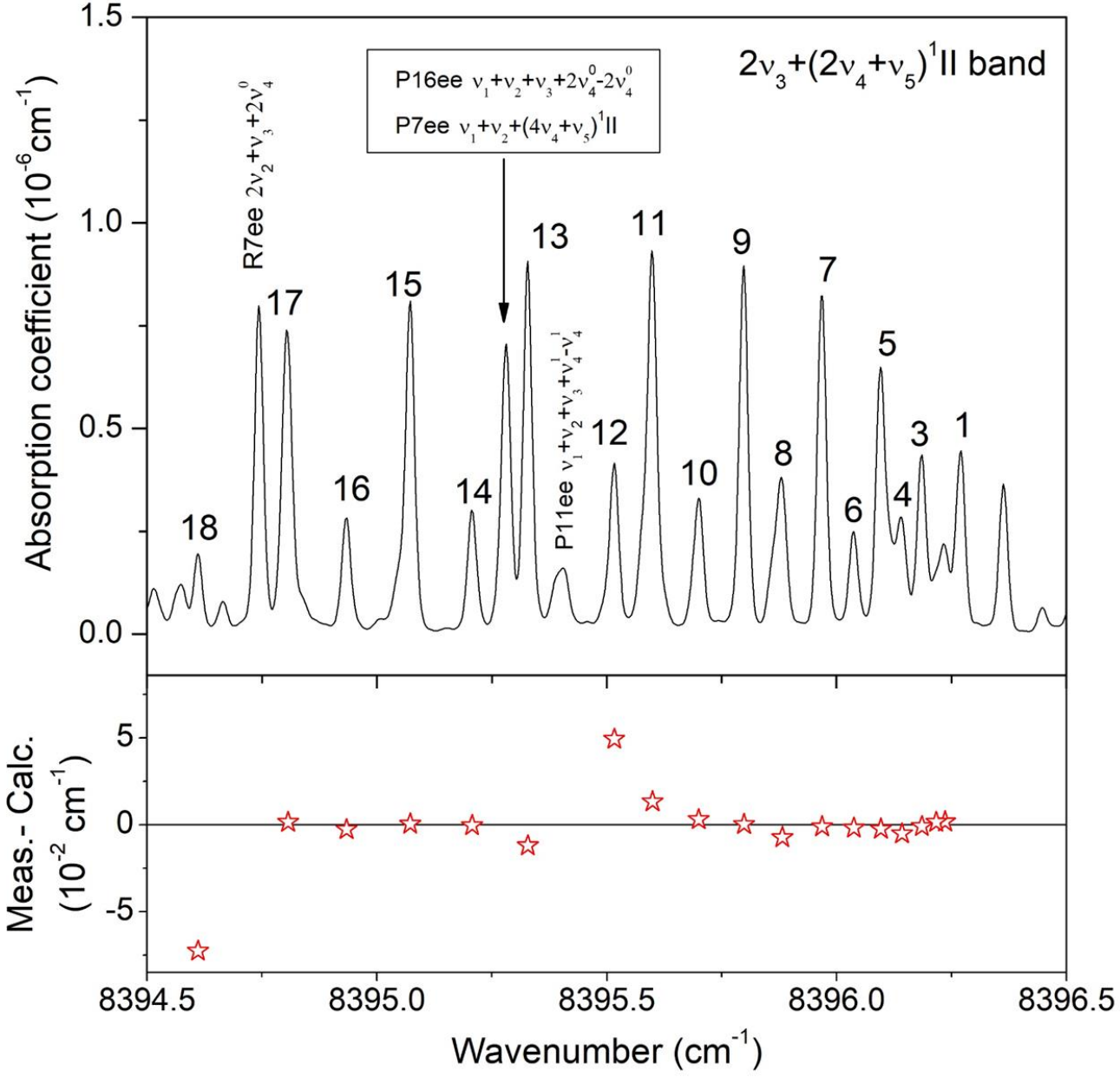
Absorption coefficient (10^{-6}cm^{-1})
1.5
1.0
0.5
0.0
P16ee $\nu_1+\nu_2+\nu_3+2\nu_4^0-2\nu_4^0$
P7ee $\nu_1+\nu_2+(4\nu_4+\nu_5)^1$II
$2\nu_3+(2\nu_4+\nu_5)^1$II band
R7ee $2\nu_2+\nu_3+2\nu_4^0$
P11ee $\nu_1+\nu_2+\nu_3+\nu_4^1-\nu_4^1$
18
17
16
15
14
13
12
11
10
9
8
7
6
5
4
3
1
Meas.- Calc. (10^{-2} cm^{-1})
5
0
-5
8394.5
8395.0
8395.5
8396.0
8396.5
Wavenumber (cm^{-1})

Fig. 8

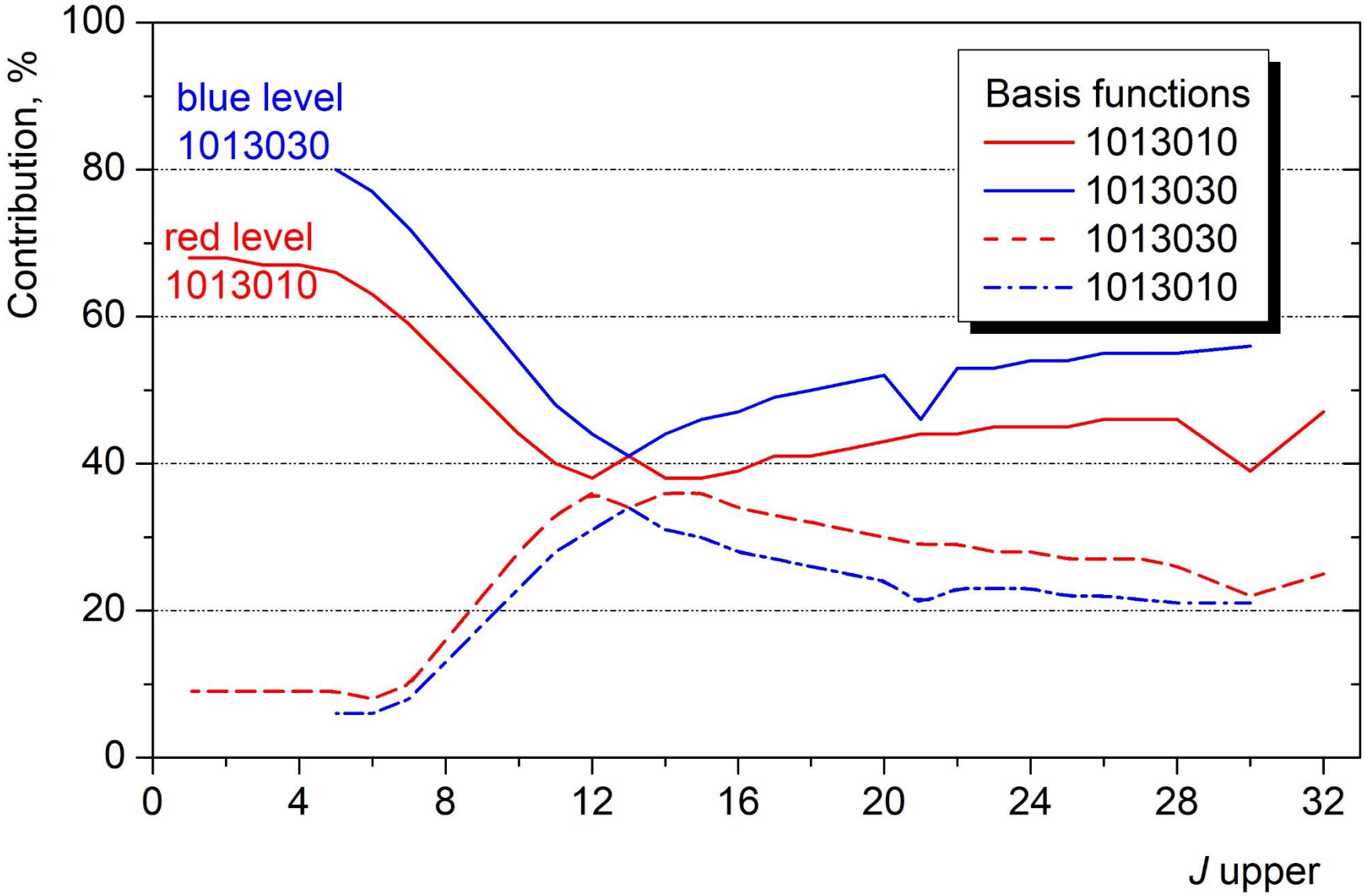
Contribution, %
100
80
60
40
20
0
0
4
8
12
16
20
24
28
32
J upper
blue level
1013030
red level
1013010
Basis functions
1013010
1013030
1013030
1013010

Fig. 9

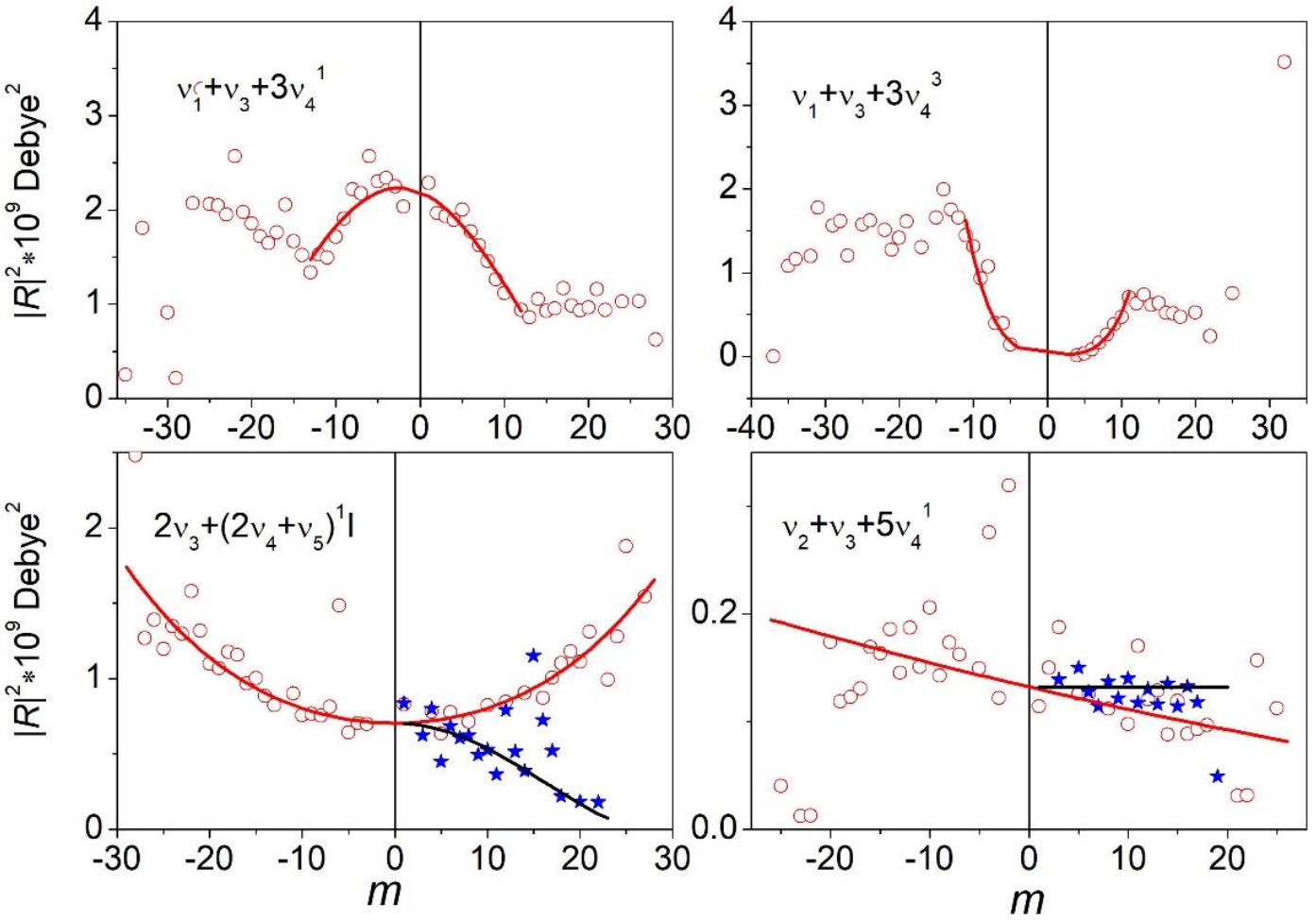
$\nu_1+\nu_3+3\nu_4^1$
$\nu_1+\nu_3+3\nu_4^3$
$2\nu_3+(2\nu_4+\nu_5)^1$I
$\nu_2+\nu_3+5\nu_4^1$
$|R|^2*10^9$ Debye^2
m

Fig. 10

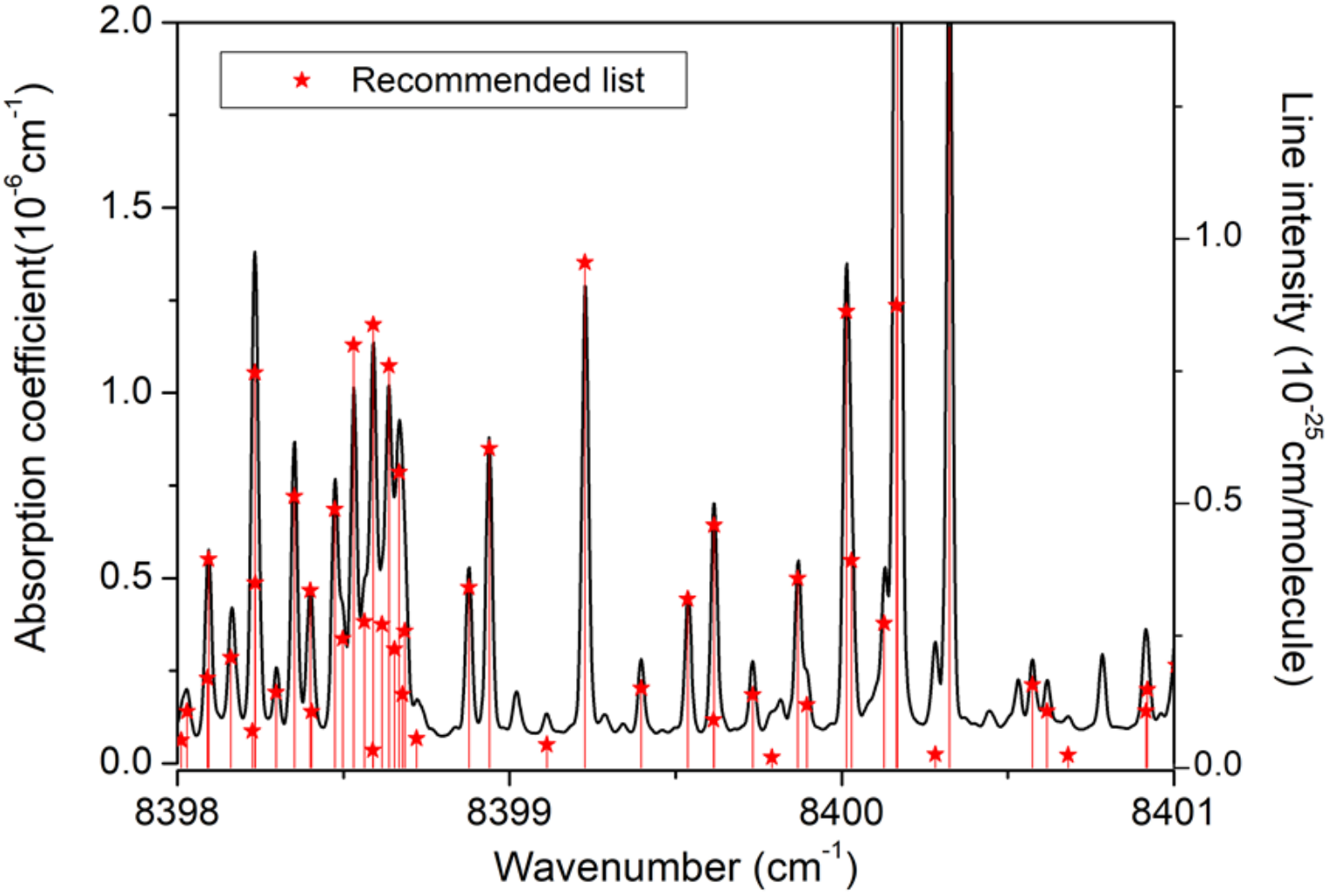
Recommended list
Absorption coefficient(10^{-6}cm^{-1})
Line intensity (10^{-25}cm/molecule)
Wavenumber (cm^{-1})
2.0
1.5
1.0
0.5
0.0
1.0
0.5
0.0
8398
8399
8400
8401

Conflict of Interest

The authors declare that they have no known competing financial interests or personal relationships that could have appeared to influence the work reported in this paper.

O. Lyulin: investigation; **S. Kassi** : investigation; **A Campargue**: investigation